ATMOSPHERIC TRANSPORT OF HYDROGEN SULFIDE FROM PROPOSED GEOTHERMAL POWER PLANTS (UNITS 13, 14, 16 AND 18) FOR THE WEST WIND DIRECTION

Predictions by Physical Modeling
in a Wind Tunnel

by

R. L. Petersen* and J. E. Cermak**

Prepared for

Pacific Gas and Electric Company
San Francisco, California

Fluid Dynamics and Diffusion Laboratory
Fluid Mechanics and Wind Engineering Program
Colorado State University
Fort Collins, Colorado 80523

November 1977

CER77-78RLP-JEC10

*Graduate Research Assistant, Department of Civil Engineering
**Director, Fluid Dynamics and Diffusion Laboratory

ABSTRACT

Tests were conducted in the Colorado State University environmental wind tunnel facility of the transport and dispersion of the H_2S plume emanating from cooling towers positioned at four locations in the Geysers area.

The wind tunnel tests were conducted with the cooling towers and terrain modeled to a scale of 1:1920. Ground-level concentrations were measured in the vicinity of Anderson Springs for selected wind speeds and one wind direction. Ground-level concentration patterns were established for each test condition studied. Data obtained include photographs and motion pictures of smoke plume trajectories as well as ground-level tracer gas concentrations downwind of the cooling towers.

ACKNOWLEDGMENTS

Mr. James A. Garrison supervised construction of the terrain model and photographic recording of the flow visualizations. Mr. Nisim Hazan collected and processed the velocity data, and Mr. James Maxton assisted in collecting the concentration and velocity data. Mr. John Elmer's help in the data collection and data reduction phase of the project is also greatly appreciated. Mrs. Debbie Bonser typed the manuscript.

TABLE OF CONTENTS

LIST OF TABLES

LIST OF FIGURES

LIST OF SYMBOLS

Symbol	Definition	Dimensions
D	Stack diameter	(L)
E	Gas chromatograph response	(mvs)
Fr	Froude number $\frac{V^2}{g(\frac{\Delta\rho}{\rho_a})\ D}$	(-)
g	Gravitational constant	(L/T^2)
h	Cooling tower height	(L)
H	Height of terrain above cooling tower elevation	
k	von Karman constant	(-)
K	Concentration isopleth	(-)
L_o	Distance from beginning of wind tunnel	(L)
Q_s	Source strength	(M/T)
R	Exhaust velocity ratio V_s/V_a	(-)
Re_{L_o}	Reynolds number $\frac{VL_o}{\nu}$	(-)
U_*	Friction velocity	(L/T)
V	Mean velocity	(L/T)
x,y	General coordinates--downwind, lateral	(L)
z_o	Surface roughness parameter	(L)

Symbol	Definition	Dimensions
(Greek Symbols)		
χ	Local concentration	(M/L^3 or ppm)
τ	Sampling time	(T)
θ	Azimuth angle of upwind direction measured from plant north	(-)
σ	Standard deviation of either plume dispersion or wind angle fluctuations	(L) (-)
ν	Kinematic viscosity	(L^2/T)
δ	Boundary layer thickness	(L)
γ	Specific weight	(M/T^2L^2)
ρ	Density	(M/L^3)
Ω	Angular velocity	(1/L)
μ	Dynamic viscosity	M/(TL)
Λ	Volume flow rate	(L^3/T)
(Subscripts)		
a	Meteorological tower	
s	Stack	
m	Model	
p	Prototype	
max	Maximum	
g	Geostrophic or gradient wind	
rms	Root mean square	
∞	Reference value	
FS	Free stream	

CONVERSION TABLE

(English to Metric Units)

Multiply Units	by	To Obtain
inches	2.540	centimeters
square inches	6.452	square centimeters
cubic inches	16.39	cubic centimeters
feet	0.3048	meters
square feet	0.0929	square meters
cubic feet	0.02832	cubic meters
feet/second	0.3048	meters/second
miles/hour	0.4470	meters/second
cubic feet/minute	0.02832	cubic meters/minute
cubic feet/minute	0.00047	cubic meters/second

1.0 INTRODUCTION

The purpose of this study was to determine the transport characteristics of hydrogen sulfide (H_2S) released in plumes emanating from four cooling towers (Units 13, 14, 16 and 18) in the Geysers Geothermal Area. The location of these cooling towers is shown in Figure 1.1 in relation to Anderson Springs and Whispering Pines. Using 1:1920 scale models of the cooling towers and surrounding topography in a wind tunnel the dispersion characteristics were studied for the west wind direction. For this wind direction the units are approximately in a line which could result in the highest combined H_2S impact in the populated area of Anderson Springs.

Downwind ground-level H_2S concentrations were determined by sampling tracer gases (propane, ethane, methane and butane) released from the model cooling towers. Overall plume geometry was obtained by photographing the plumes made visible by releasing smoke (titanium tetrachloride) from the model cooling towers.

The primary focus of this study was on the H_2S concentrations in the vicinity of Anderson Springs for neutral thermal stratification. Studies of the ridgeline and free air winds were confined to the 270^{o} azimuth. Figures 1.2a and b show the wind roses which were obtained from meteorological towers at Units 7 and 8, Station 6 and in the vicinity of Anderson Ridge, Station 2. Information from the ridge line meteorological station (Station 2) indicated that winds in the sector 270^{o} occur approximately 9 percent of the time. Wind speeds of 2.5, 4.1, 7.8 and 10.9 m/s at meteorological station #2 were modeled to obtain representative concentrations under beneficial and adverse plume rise conditions.

Included in this report are a brief description of the similarity requirements for atmospheric motion, an explanation of test methodology

and procedures, results of plume visualization and concentration measurements, and results of wind flow measurements.

This report is supplemented by a motion picture (in color) which shows plume behavior for the various wind speeds studied. Black and white photographs as well as slides of each plume visualization further illustrate the material presented.

2.0 SIMULATION OF ATMOSPHERIC MOTION

The use of wind tunnels for model tests of gas diffusion by the atmosphere is based upon the concept that nondimensional concentration coefficients will be the same at corresponding points in the model and the prototype and will not be a function of the length scale ratio. Concentration coefficients will only be independent of scale if the wind tunnel boundary layer is made similar to the atmospheric boundary layer by satisfying certain similarity criteria. These criteria are obtained by inspectional analysis of physical statements for conservation of mass, momentum, and energy. Detailed discussions have been given by Halitsky (1963), Martin (1965), and Cermak et al. (1966). Basically, the model laws may be divided into requirements for geometric, dynamic, thermic, and kinematic similarity. In addition, similarity of upwind flow characteristics and ground boundary conditions must be achieved. A detailed discussion of the similarity requirements for this study is found in Cermak and Petersen (1977) and will not be repeated here.

To summarize, the following scaling criteria were applied for the neutral boundary layer situation:

1. $Fr = \dfrac{\rho_a V_a^2}{\Delta\gamma D}$; $(Fr)_m = (Fr)_p$,

2. $R = \dfrac{V_s}{V_a}$; $R_m = R_p$,

3. $L_o/K_s > 300$ (implies Reynolds number independence),

4. $(z_o)_m = (z_o)_p$,

5. Similar geometric dimensions, and

6. Similar velocity and turbulence profiles upwind.

3.0 TEST APPARATUS

3.1 Wind Tunnels

The environmental wind tunnel (EWT) shown in Figure 3.1 was used for this neutral flow study. This wind tunnel, especially designed to study atmospheric flow phenomena, incorporates special features such as adjustable ceiling, rotating turntables, transparent boundary walls, and a long test section to permit adequate reproduction of micro-meteorological behavior. Mean wind speeds of 0.06 to 37 m/s (0.14 to 80 miles/hour) in the EWT can be obtained. In the EWT, boundary layers four feet thick over the downstream 12.2 meters can be obtained with the use of vortex generators at the test section entrance. The flexible test section roof on the EWT is adjustable in height to permit the longitudinal pressure gradient to be set at zero.

3.2 Model

The cooling towers were modeled at a scale of 1:1920. The relevant building dimensions are given in Table 2.1 and a photograph of one of the four identical models is shown in Figure 3.2-1.

Topography was modeled to the same scale by cutting Styrofoam sheets of 9.6 cm and 1.27 cm thicknesses to match contour lines of a topographic map enlarged to the 1:1920 scale. The scale model of the topography is shown mounted in the wind tunnel in Figure 3.2-2. The model terrain was not smoothed so as to increase the surface roughness and thereby prevent the formation of a laminar sublayer. This increased roughness also contributed toward achieving Reynolds number independence of flow over the test section.

An array of sampling tubes was inserted into the model terrain to give a minimum of 33 representative sampling locations. The sampling locations are shown in Figure 5.1 and enumerated in Table 5.1.

Metered quantities of gas were allowed to flow from the cooling tower to simulate the exit velocity. Helium, compressed air, and propane (the tracer) were mixed to give the highest practical specific weight. Fischer-Porter flow meter settings were adjusted for pressure, temperature, and molecular weight effects as necessary. When a visible plume was required, the gas was bubbled through titanium tetrachloride before emission.

3.3 Flow Visualization Techniques

Smoke was used to define plume behavior from the four geothermal power plants. The smoke was produced by passing the air mixture through a container of titanium tetrachloride located outside the wind tunnel and transported through the tunnel wall by means of a tygon tube terminating at the cooling tower inlet. A schematic of the process is shown in Figure 3.3-1.

The plume was illuminated with arc-lamp beams and a visible record was obtained by means of pictures taken with a Speed Graphic camera. Additional still pictures were obtained with a Hasselblad camera. Stills were taken with a camera speed of one second to identify mean plume boundaries. A series of 16 mm color motion pictures was also taken with a Bolex motion picture camera.

3.4 Gas Tracer Technique

After the desired tunnel speed was obtained, a mixture of propane, helium, and air of predetermined concentration was released from the cooling tower at the required rate to simulate prototype plume rise. Samples of gas were withdrawn from the sample points and analyzed. The flow rate of propane mixture was controlled by a pressure regulator at

the supply cylinder outlet and monitored by a Fischer-Porter precision flow meter. The sampling system is shown in Figure 3.4-1.

A more complete discussion of the gas sampling and analysis techniques is given in Cermak and Petersen (1977). All concentration data presented herein are in dimensionless form. Appendix A enumerates the procedures for converting the data to prototype concentrations.

3.5 Wind Profile Measurements

The following instruments were used during the course of this study to measure velocity:

1. Pitot tube--used for freestream velocity and velocity profile measurements.
2. Thermo System (TSI model 1050) constant temperature hot-film anemometer--used for low speed measurements close to surface of model.

The use of a pitot tube for velocity measurements* entails measuring the difference between total and static pressure. The velocity is calculated by the relationship

$$V = K' \sqrt{\frac{T}{P_{AT}} \Delta P}$$

V - velocity

K' - proportionality coefficient

T - absolute air temperature

P_{AT} - atmospheric pressure

ΔP - the difference between total and static pressure

The pressure difference was measured with a MKS Baratron Type 77.

*Detailed discussion on pitot tube and hot-wire anemometry can be found in textbooks. Only those concepts that are essential to our measurements are presented here.

Calibration of the TSI hot-film anemometer was carried out with a TSI calibrator. The calibration measurements were correlated to King's law and put in the following form:

$$E^2 = A + BV^n$$

where

E = the output signal of the wire (mv)

V = the velocity sensed (m/s)

n, A and B = the constants of King's law

The coefficients A, B, and n for the velocity range from .25 to 25 m/s were found to be

A = 4.40

B = 2.082

n = 0.50

King's law fit to the calibration of the hot film is shown in Figure 3.5-1.

To obtain the velocity profiles a calibrated carriage was used together with a digital voltmeter. In this manner, the location of the anemometer or pitot tube over the terrain could be adjusted from outside the tunnel.

To set the wind tunnel conditions the velocity at meteorological Station 2 (.52 cm above the modeled terrain) was correlated to the upwind freestream velocity. The velocity at the meteorological station was measured with the TSI hot-film anemometer while the freestream velocity was measured with a pitot tube. The curve relating the two (the meteorological station versus freestream) is shown in Figure 3.5-2. Thus the desired speed at meteorological Station 2 was obtained by varying the freestream velocity.

4.0 TEST PROGRAM RESULTS - VISUALIZATION

The visualization test results consist of photographs and movies showing the plume behavior for Units 13, 14, 16 and 18 for the west wind direction and four wind speeds. The photographs and movies were taken while smoke was released simultaneously from all four units.

The sequence of photographs in Figure 4.1 shows the combined plume behavior for the 270° wind direction and wind speeds at meteorological tower height (10 m, AGL) of 2.5, 4.1, 7.8 and 10.9 m/s. For the light wind speed cases (2.5 m/s) the plumes remain elevated over Anderson Springs. However, as the wind speed increases, the plume altitude decreases, and for the high wind speed cases, the plume tends to follow along the terrain confluences. For wind speeds of 4.1 m/s or greater the plumes emanating from the cooling towers appear to flow along the terrain at a relatively low effective plume altitude.

Complete sets of still photographs supplement this report. Color motion pictures have been arranged into titled sequences and the sets available are given by run number in Table 4.1-1.

5.0 TEST PROGRAM RESULTS - CONCENTRATION MEASUREMENTS

The diffusion of gaseous effluent from the four model cooling towers was studied for one wind direction (270° azimuth) and four wind speeds. A different tracer material was released from each model cooling tower (propane from Unit 13, ethane from Unit 14, methane from Unit 18 and n-butane from Unit 16) and concentrations of the tracer were measured at 33 locations in the vicinity of Anderson Springs. The sampling array is shown in Figure 5.1 and prototype locations for all sampling points are summarized in Table 5.1. The zero coordinate is represented by the base of the wind direction arrow in all figures.

All concentration data have been reported in dimensionless form as explained in Cermak and Petersen (1977). To convert from a dimensionless concentration coefficient, K, to a prototype H_2S concentration, refer to the procedures outlines in Appendix A.

The concentration results are summarized for Units 13, 14, 16 and 18 in Tables 5.2 through 5.5. Sample locations in the tables are defined in Table 5.1 and Figure 5.1.

In order to visually and quantitatively assess the effect of wind speed on ground level concentration patterns for this wind direction, Figures 5.2 through 5.5 were prepared. These figures show isopleths of the dimensionless concentration coefficient, K, for each unit and wind speed studied. The maximum nondimensional concentration occurs with either a 7.8 or 10.9 m/s wind speed depending upon the unit location.

The highest K-values near Anderson Springs for each unit are approximately

- Unit 13 - 10 (10.9 m/s)
- Unit 14 - 4 (10.9 m/s)
- Unit 16 - 5 (7.8 m/s)
- Unit 18 - 5 (10.9 m/s)

6.0 TEST RESULTS - VELOCITY MEASUREMENTS

This section discusses the results of the velocity measurements. Techniques for data collection are described in Section 3.5. Velocity measurements were obtained to meet the following objectives.

- Provide a relation between the freestream velocity and the velocity at the ridgeline meteorological tower (Station 2).
- Present velocity profiles above Meteorological Station 2, Unit 14, Unit 18 and over Anderson Springs.

Figure 6.1 shows the velocity profiles at the four sites mentioned above. Further information on the velocity measurements is given in Cermak and Petersen (1977). The relation between freestream velocity and the velocity at the meteorological tower is discussed in Section 3.5.

REFERENCES

Cermak, J. E. and J. Peterka, "Simulation of Wind Fields over Point Arguello, California, by Wind-Tunnel Flow over a Topographical Model," Final Report, U.S. Navy Contract N126(61756)34361 A(PMR), Colorado State University, CER65JEC-JAP64, December 1966.

Cermak, J. E. and R. L. Petersen, "Atmospheric Transport of Hydrogen Sulfide from Proposed Geothermal Power Plant (Unit 16) Predictions by Physical Modeling in a Wind Tunnel," Colorado State University, CER76-77JEC-RLP47, March 1977.

Halitsky, J., "Gas Diffusion near Buildings," Geophysical Sciences Laboratory Report No. 63-3, New York University, February 1963.

Martin, J. E., "The Correlation of Wind Tunnel and Field Measurements of Gas Diffusion Using Kr-85 as a Tracer," Ph.D. Thesis, MMPP 272, University of Michigan, June 1965.

APPENDIX A

Method for Calculating Prototype Concentrations From Nondimensional Concentration Coefficient K

- Basic Equation:

$$K = \frac{\chi V_a D^2}{\Lambda Q_s} \quad \text{Prototype}$$

where

$K \equiv$ nondimensional concentration coefficient from wind tunnel study

$\chi \equiv H_2S$ concentration (ppm)

$V_a \equiv$ wind speed at the meteorological station (m/s)

$D \equiv$ cell diameter (equal to 8.5 m)

$\Lambda \equiv$ total volume flow (use 4313 m^3/s)

$Q_s \equiv$ equivalent H_2S concentration in the incoming stack gas [(ppm) (1 - fraction removed)]

- Now solving for $\chi_{prototype}$:

$$\chi_{prototype} = K \frac{\Lambda Q_s}{V_a D^2}$$

$$= 59.7 \frac{KQ_s}{V_a}$$

- Example:

let $K = 20 \times 10^{-5}$

$Q_s = 10$ ppm

$V_a = 9.8$ m/s

then $\chi_{prototype} = \frac{(59.7)\ (20 \times 10^{-5})\ (10)}{9.8} = 0.012$ ppm

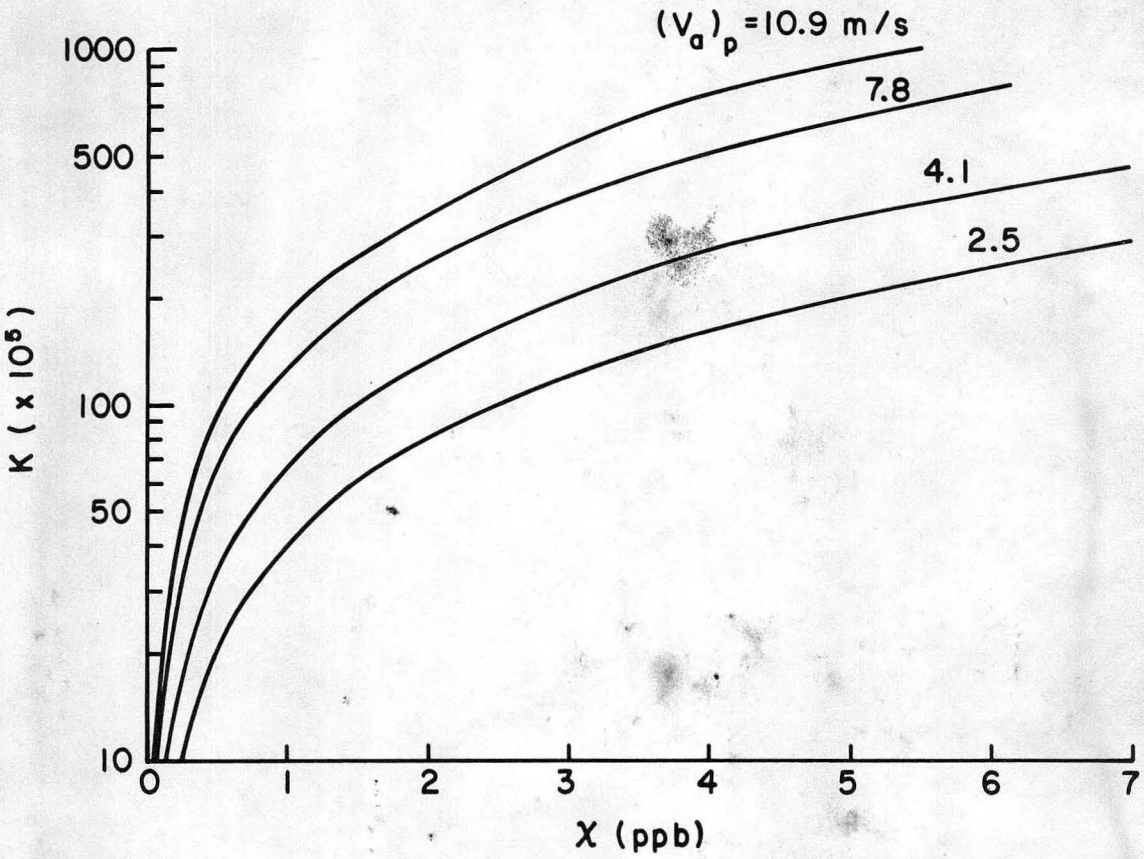

Figure A-1. Concentration, χ(ppb) versus nondimensional concentration coefficient K for an input steam concentration equivalent to 1 ppb H_2S.

TABLES

Table 2.1 Model and Prototype Dimensional Parameters
Units 13, 14, 16, and 18

	Parameter	Prototype	Model
1.	Building		
	a. length (ℓ)	98 m	5.1 cm
	b. width (w)	21.5 m	1.1 cm
	c. height (h)	20 m	1.0 cm
2.	Exit Temperature (T_s)	319°K	293°K
3.	Cell Diameter (D)	8.5	0.44 cm
4.	Number of Cells	10	10
5.	Exit Velocity (V_s)	7.6 m/s	0.49 m/s
6.	Volumetric Emission Rate (Λ)	4312.6 m^3/s	74.51 cc/s
7.	Gas Density (ρ_a)	0.97 kg/m^3	0.21 kg/m^3
8.	Ambient Density (ρ_a)	1.08	1.02
9.	Wind Speed at Meteorological Tower (V_a)	2.5, 4.1, 7.8, 10.9 m/s	0.16, 0.26, 0.50, 0.70 m/s
10.	Wind Direction	West	West
11.	Surface Roughness (z_o)	0.5 m	0.02 cm
12.	Ambient Pressure	900 mb	850 mb
13.	Ambient Temperature	293°K	293°K
14.	Virtual Temperature Increment	2.92°C	N/A

Table 2.2 Model and Prototype Dimensionless Parameters
Units 13, 14, 16, and 18

Parameter	Prototype	Model
$\frac{\delta_a}{H}$	1.84	2.15
$\frac{z_o}{H}$	2.0×10^{-3}	1.5×10^{-3}
$\frac{D}{H}$	3.5×10^{-2}	3.5×10^{-2}
$\frac{h}{H}$	1.6×10^{-2}	1.6×10^{-2}
$R = \frac{V_s}{V_a}$	3.0, 1.9, 0.97, 0.70	3.1, 1.9, 0.98, 0.70
$Fr = \frac{\rho_a V_a^2}{g(\rho_a - \rho_s)D}$	0.75, 2.02, 7.30, 14.26	0.75, 1.98, 7.34, 14.38
$DR = \frac{\rho_a - \rho_s}{\rho_a}$	0.10	0.79

Table 4.1 Summary of Photographs Taken for Units 13, 14, 16 and 18

Photo or Run No.	Wind Direction	Wind Speed (m/s)
1	270°	2.5
2	270°	4.1
3	270°	7.8
4	270°	10.9

Table 5.1 Prototype Sampling Location Key and Site Location Key

	x-Coordinate (m)	y-Coordinate (m)	Elevation (m, MSL) (m)
1	2268	2463	546
2	2268	1890	442
3	2262	1232	418
4	2274	927	430
5	2256	616	451
6	2256	-55	537
7	2268	-610	671
8	2091	2457	537
9	2085	1835	439
10	2098	1232	433
11	2091	927	410
12	2104	610	439
13	2085	-31	463
14	2110	-610	671
15	1770	2463	518
16	1770	1896	482
17	1777	1232	439
18	1787	915	418
19	1793	619	418
20	1791	-58	476
21	1791	-652	628
22	1505	2470	522
23	1505	1896	515
24	1524	1262	470
25	1543	915	424
26	1562	610	512
27	1543	-61	445
28	1562	-671	573
29	1195	2500	604
30	1220	1970	532
31	1220	1256	488
32	1244	884	425
33	1244	585	517
34	1238	-61	500
35	1268	-671	561
36	823	2506	634
37	811	1939	559
38	823	1274	500
39	829	915	439
40	854	567	535
41	848	-55	622
56	848	-671	628
42	488	2470	668
43	500	1921	598
44	470	1207	488
45	470	927	473
46	457	592	512
47	518	-24	723
48	457	-671	689
49	0	2470	681
50	0	1896	601
51	0	1220	616
52	0	915	555
53	0	598	561
55	0	-695	738

Sites	x	y	Elevation
13	-1482	726	982
14	-6037	2220	573
16	409	-49	720
18	-2488	213	830

Table 5.2 Nondimensional Concentration Coefficients ($\times 10^5$) for Unit 13

Location Number	Wind Speed (m/s)			
	2.5	4.1	7.8	10.9
2	0.00	0.00	0.00	0.00
3	0.34	0.20	0.00	0.00
4	1.68	1.57	2.81	3.14
5	1.23	2.68	6.77	7.48
6	0.33	3.45	0.00	4.93
9	0.00	0.00	0.00	0.00
10	0.13	0.36	0.00	0.00
11	1.95	1.84	1.65	1.74
12	1.30	2.72	6.84	7.44
13	0.10	3.91	4.50	3.52
16	0.00	0.00	0.51	0.00
17	0.19	0.19	0.00	0.00
18	2.19	2.14	2.09	2.83
19	1.59	3.57	6.07	7.90
20	0.04	3.31	3.28	2.78
23	0.00	0.00	0.00	0.00
25	1.58	2.06	3.35	3.45
26	1.54	1.01	3.23	3.82
27	0.00	2.84	1.36	2.12
31	0.00	0.00	0.00	0.14
32	0.82	0.84	1.19	2.22
33	2.89	3.37	7.87	10.73
34	0.13	2.16	3.67	5.95
37	0.00	0.00	0.00	0.00
38	0.00	0.00	0.00	0.00
39	0.57	1.35	3.25	6.54
40	3.04	5.55	9.99	12.98
41	0.17	2.90	4.43	5.49
44	0.00	0.11	0.50	0.00
45	1.22	3.05	4.19	0.00
46	2.65	7.08	13.90	3.20
51	0.00	0.00	0.00	0.03
52	0.00	0.00	0.00	0.00

Table 5.3 Nondimensional Concentration Coefficients ($\times 10^5$) for Unit 14

Location Number	Wind Speed (m/s)			
	2.5	4.1	7.8	10.9
2	0.48	0.65	0.00	0.00
3	1.71	1.71	1.30	1.36
4	1.51	2.21	2.65	2.98
5	4.19	2.27	2.94	3.56
6	0.00	1.52	0.00	2.09
9	0.67	0.67	0.15	0.00
10	1.90	2.22	1.09	1.34
11	1.59	2.56	2.30	2.53
12	0.46	2.46	2.77	3.42
13	0.00	1.82	1.72	1.61
16	1.17	0.78	0.31	0.03
17	1.73	1.87	0.75	1.29
18	1.73	2.54	2.19	3.15
19	0.48	2.19	2.73	3.34
20	0.00	1.57	1.48	1.40
23	0.98	0.91	0.31	0.24
25	1.81	2.44	2.60	2.81
26	1.71	0.83	2.49	1.98
27	0.00	1.39	0.52	0.98
31	1.98	1.93	0.98	0.16
32	1.92	2.07	2.20	2.62
33	0.90	2.28	2.95	4.56
34	0.00	1.07	1.35	2.05
37	1.30	0.65	0.11	0.00
38	1.85	0.00	0.74	0.87
39	1.87	2.04	2.48	3.70
40	1.43	2.22	3.59	4.14
41	0.01	0.99	1.53	1.81
44	0.05	1.05	0.48	0.36
45	1.57	2.26	3.15	0.00
46	1.39	2.43	3.99	3.25
51	0.72	1.25	0.32	0.10
52	0.11	0.00	0.00	0.13

Table 5.4 Nondimensional Concentration Coefficients ($\times 10^5$) for Unit 16

Location Number	Wind Speed (m/s)			
	2.5	4.1	7.8	10.9
2	0.00	0.00	0.00	0.00
3	0.00	0.00	0.00	0.00
4	0.00	0.00	0.00	0.00
5	1.70	0.23	8.11	9.72
6	7.42	3.33	0.00	32.21
9	0.00	0.00	0.00	0.00
10	0.00	0.00	0.00	0.00
11	0.00	0.00	0.00	0.00
12	1.92	0.04	8.12	13.17
13	6.60	2.51	27.55	41.17
16	0.00	0.00	0.04	0.49
17	0.00	0.00	0.00	0.00
18	0.00	0.00	0.00	0.00
19	2.60	0.55	12.88	17.87
20	6.83	3.53	33.50	54.94
23	0.00	0.00	0.26	0.04
25	0.00	0.00	0.00	0.00
26	0.60	0.00	0.77	0.62
27	2.50	4.10	40.23	53.91
31	0.00	0.00	0.00	--
32	0.00	0.00	0.00	--
33	0.00	0.00	0.00	0.00
34	4.64	3.57	45.11	71.33
37	0.00	0.00	0.40	--
38	0.04	0.00	0.01	0.26
39	0.00	0.00	0.04	0.08
40	0.00	0.00	0.00	0.04
41	0.00	6.61	50.09	78.30
44	--	0.37	0.73	0.23
45	0.00	0.00	0.21	0.38
46	0.00	0.12	0.00	0.18
51	0.11	0.00	0.00	0.53
52	0.00	0.40	0.00	0.03

Table 5.5 Nondimensional Concentration Coefficients ($\times 10^5$) for Unit 18

Location Number	Wind Speed (m/s)			
	2.5	4.1	7.8	10.9
2	0.00	0.00	0.00	0.00
3	0.07	0.17	0.00	0.00
4	0.76	0.80	1.31	1.37
5	2.15	1.61	7.50	8.72
6	1.44	4.25	0.00	13.09
9	0.00	0.03	0.00	0.00
10	0.05	0.32	0.00	0.00
11	1.20	1.12	0.71	0.74
12	1.60	1.49	6.61	8.98
13	0.74	0.00	11.20	11.43
16	0.00	0.00	0.00	0.00
17	0.08	0.14	0.00	0.00
18	1.17	1.20	0.84	1.32
19	2.08	2.66	8.52	9.60
20	0.37	4.60	10.01	10.64
23	0.00	0.00	0.05	0.00
25	0.52	0.83	1.48	1.33
26	0.48	0.66	1.46	2.64
27	0.19	4.53	5.04	9.14
31	0.00	0.05	0.00	0.02
32	0.25	0.41	0.49	0.97
33	2.26	1.67	4.06	5.23
34	1.20	5.92	10.43	16.67
37	0.00	0.17	0.04	0.00
38	0.00	0.00	0.00	0.00
39	0.29	0.45	1.61	2.31
40	2.39	2.08	4.88	6.09
41	1.68	6.29	12.62	15.95
44	0.00	0.06	0.02	0.02
45	0.31	1.05	2.03	0.00
46	2.53	4.38	6.79	1.15
51	0.00	0.04	0.08	0.35
52	0.00	0.00	0.02	0.11

FIGURES

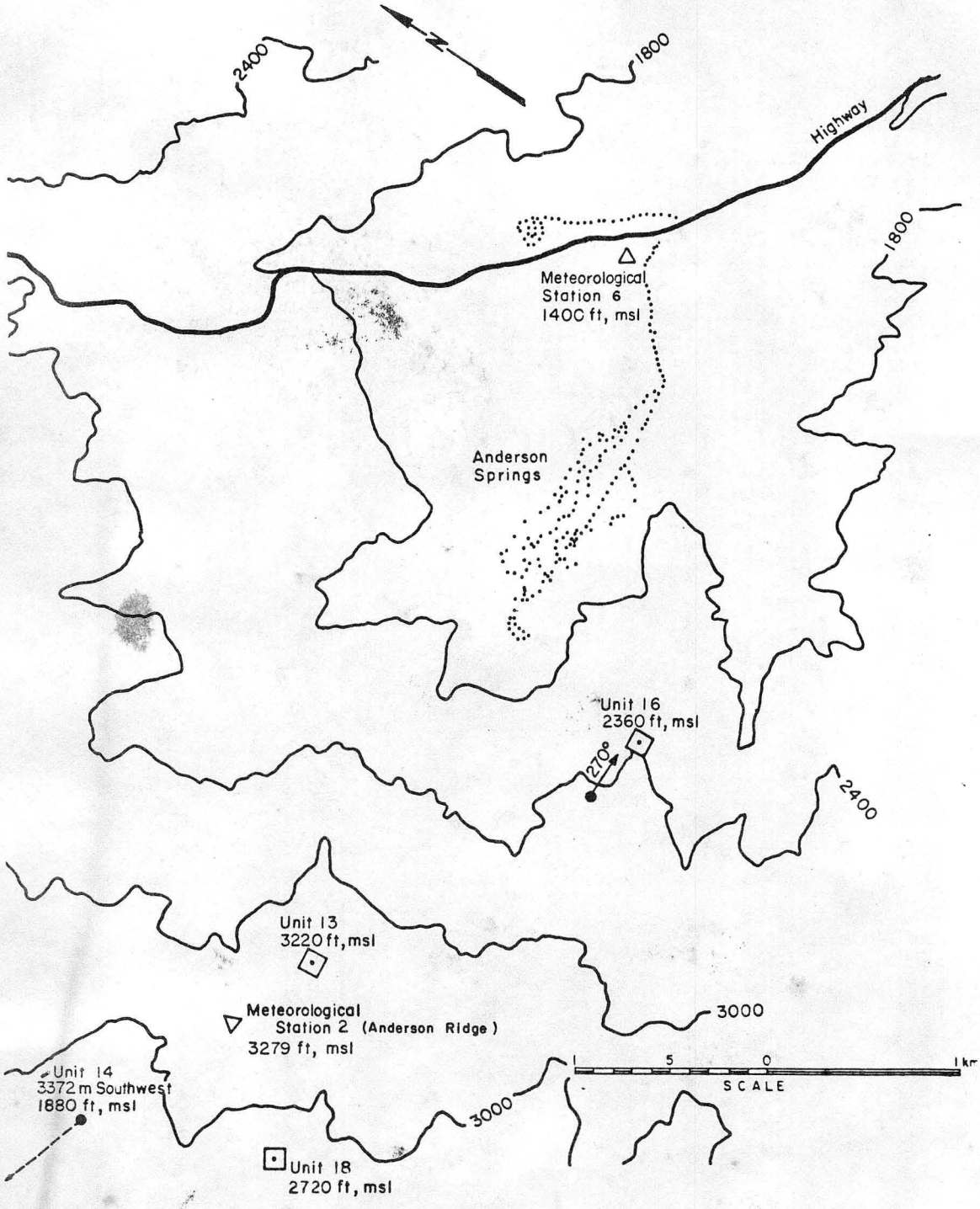

Figure 1.1. Map showing Geyser Geothermal Area and location of Units 13, 14, 16 and 18.

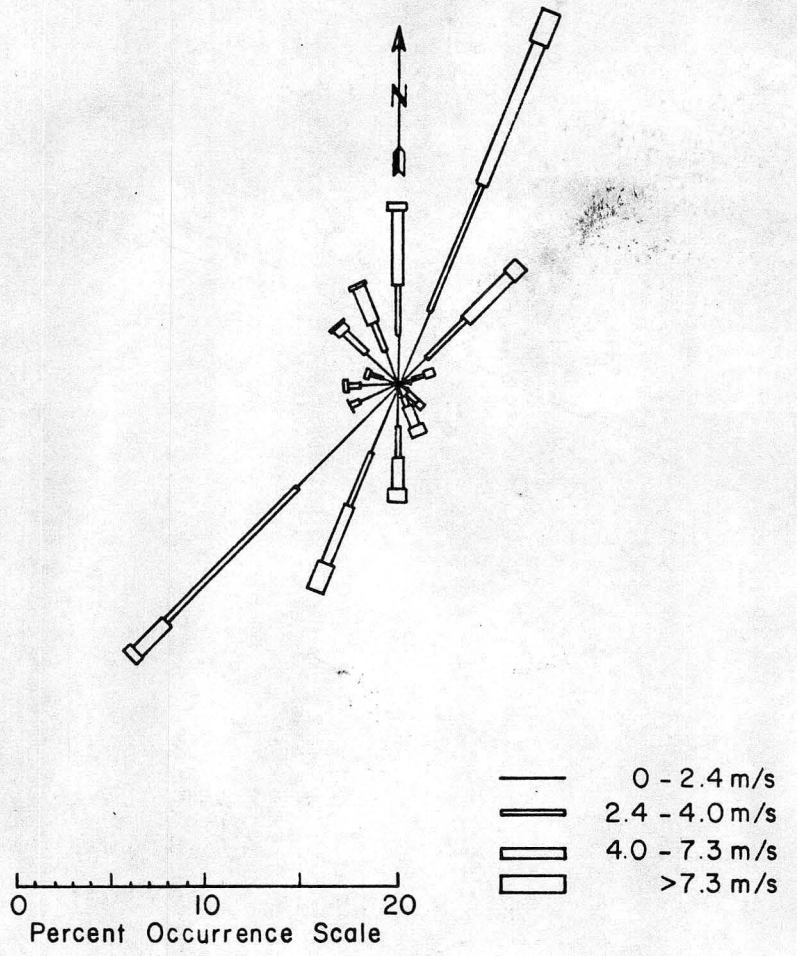

Figure 1.2a. Wind rose from meteorological Station 6, units 7 and 8.

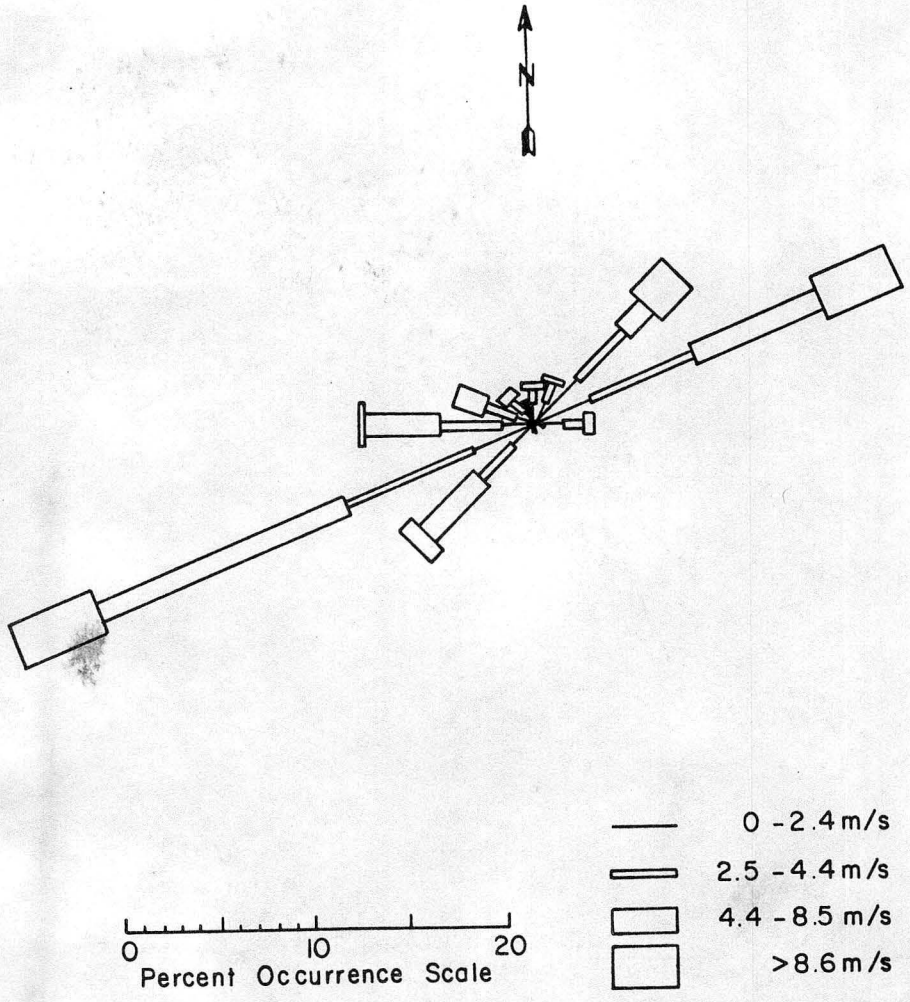

Figure 1.2b. Wind rose from meteorological Station 2, units 13 and 14.

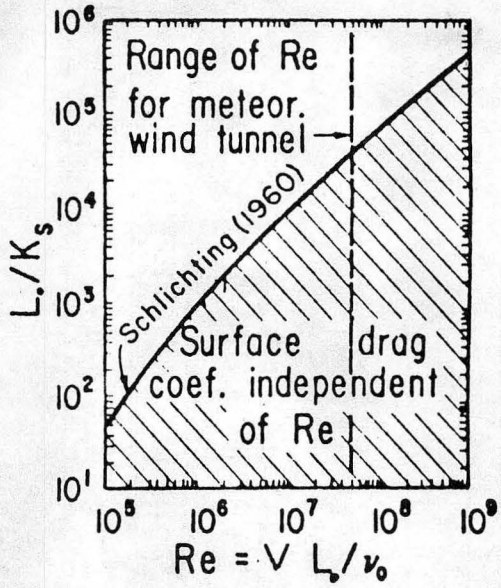

Figure 2.1. Reynolds number at which flow becomes independent of Reynolds number for prescribed relative roughness.

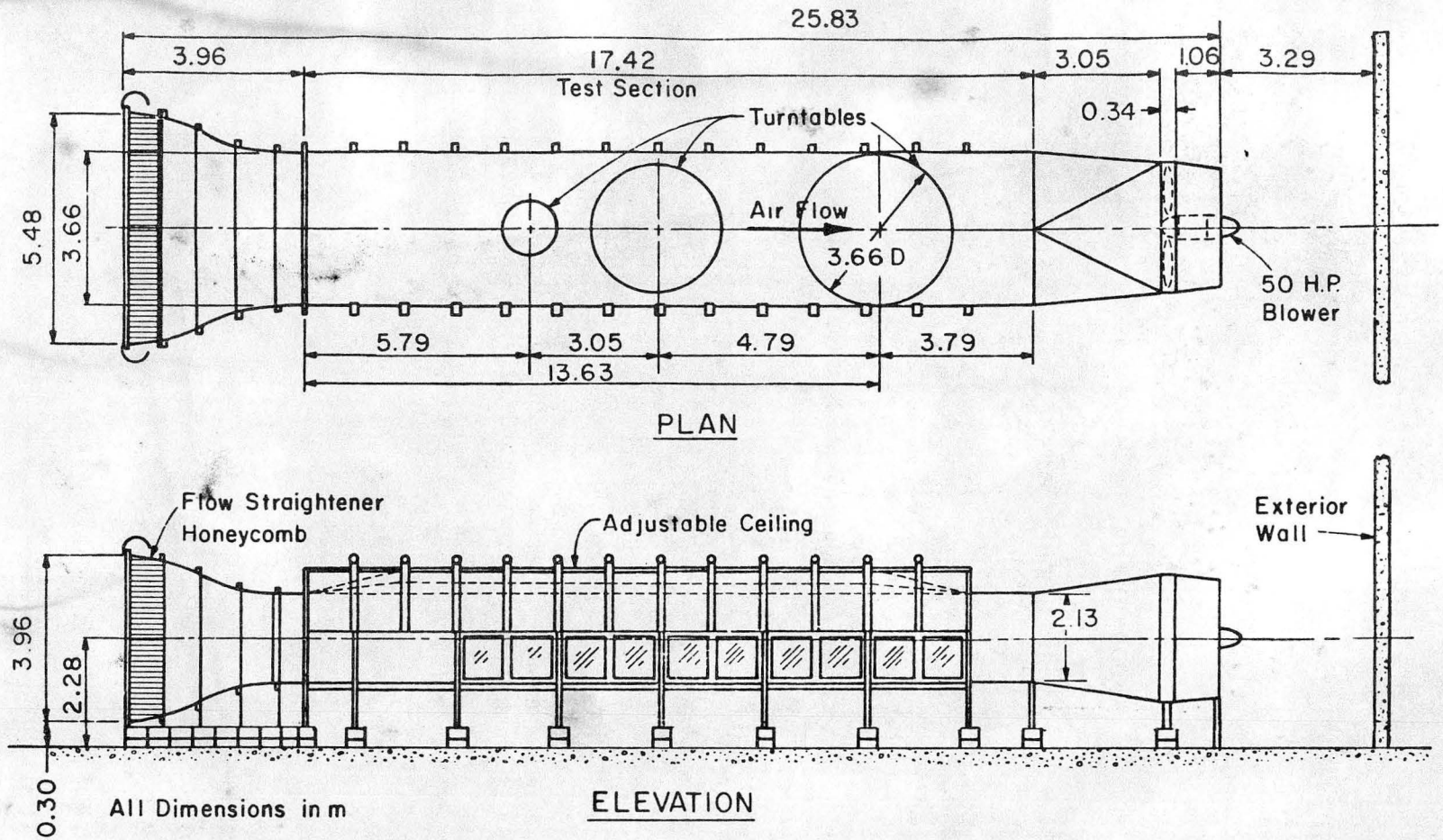

Figure 3.1. Environmental Wind Tunnel.

FLUID DYNAMICS & DIFFUSION LABORATORY
COLORADO STATE UNIVERSITY

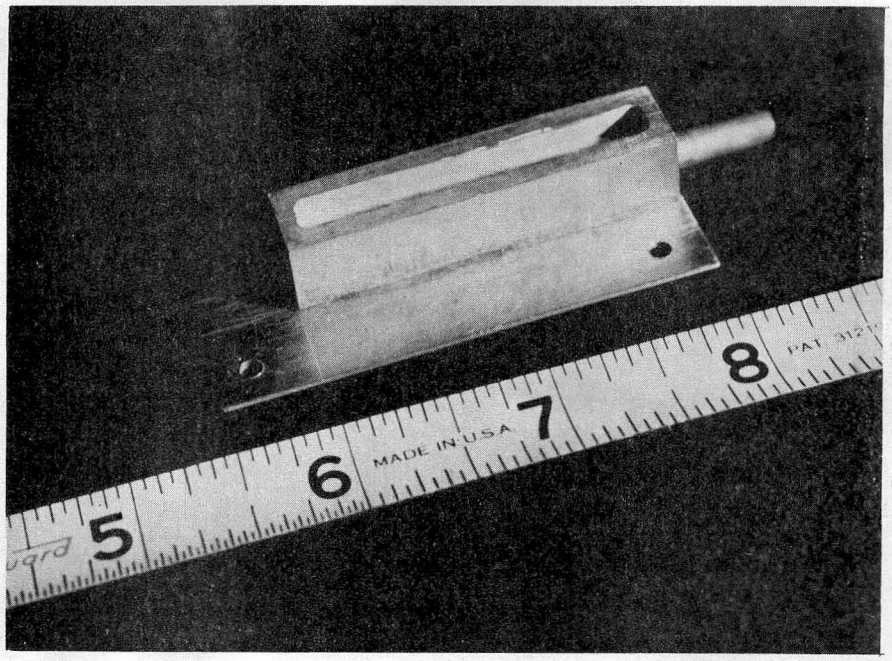

Figure 3.2-1. Photograph of cooling tower model (Scale 1:1920).

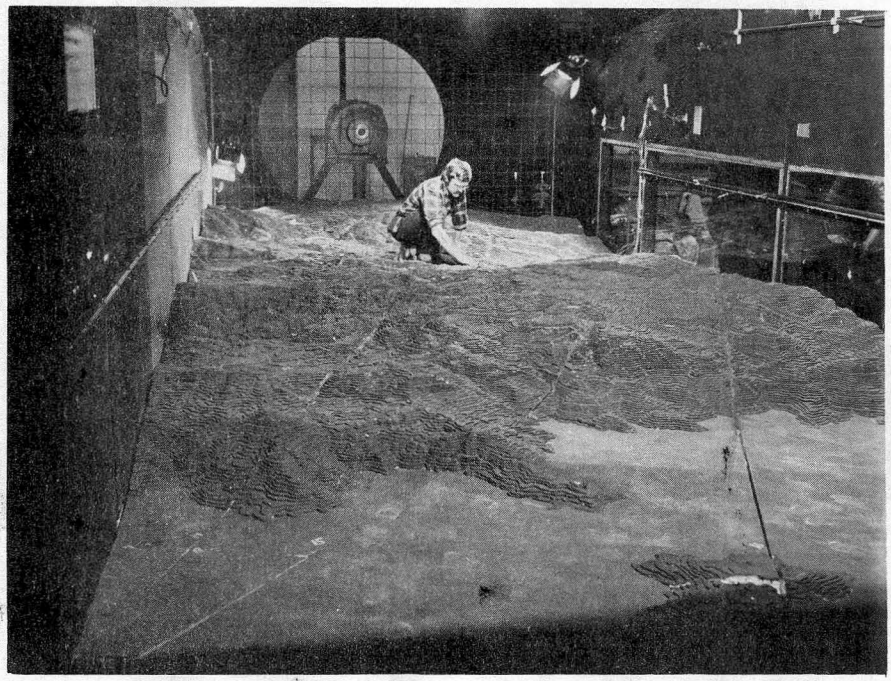

Figure 3.2-2. Photograph of terrain model in the Environmental Wind Tunnel.

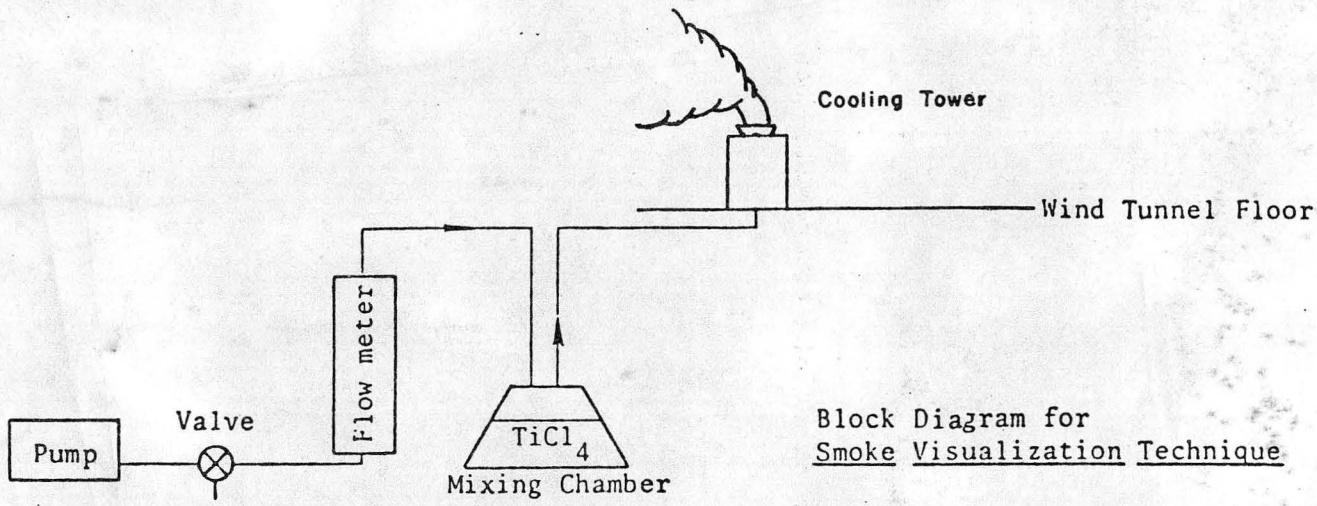

Figure 3.3-1. Schematic of plume visualization equipment.

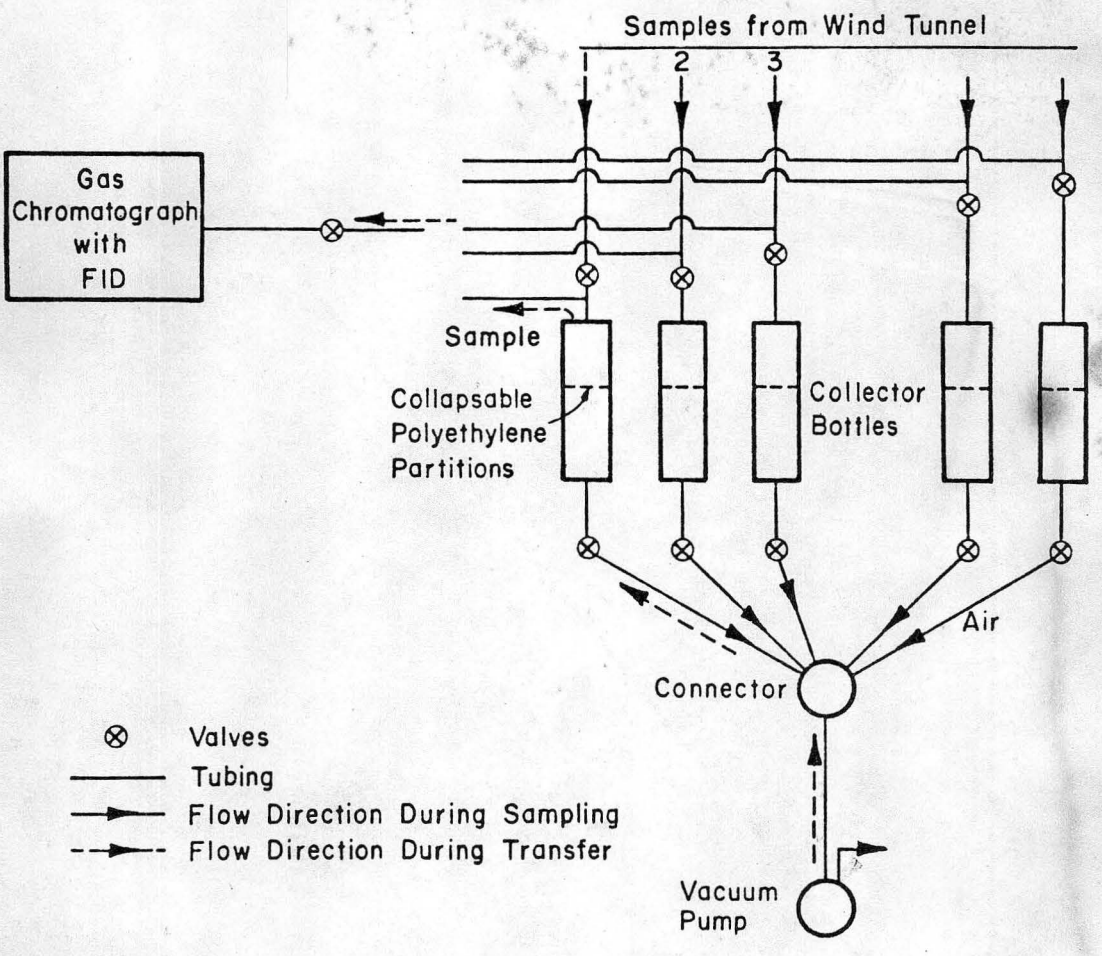

Figure 3.4-1. Schematic of tracer gas sampling system.

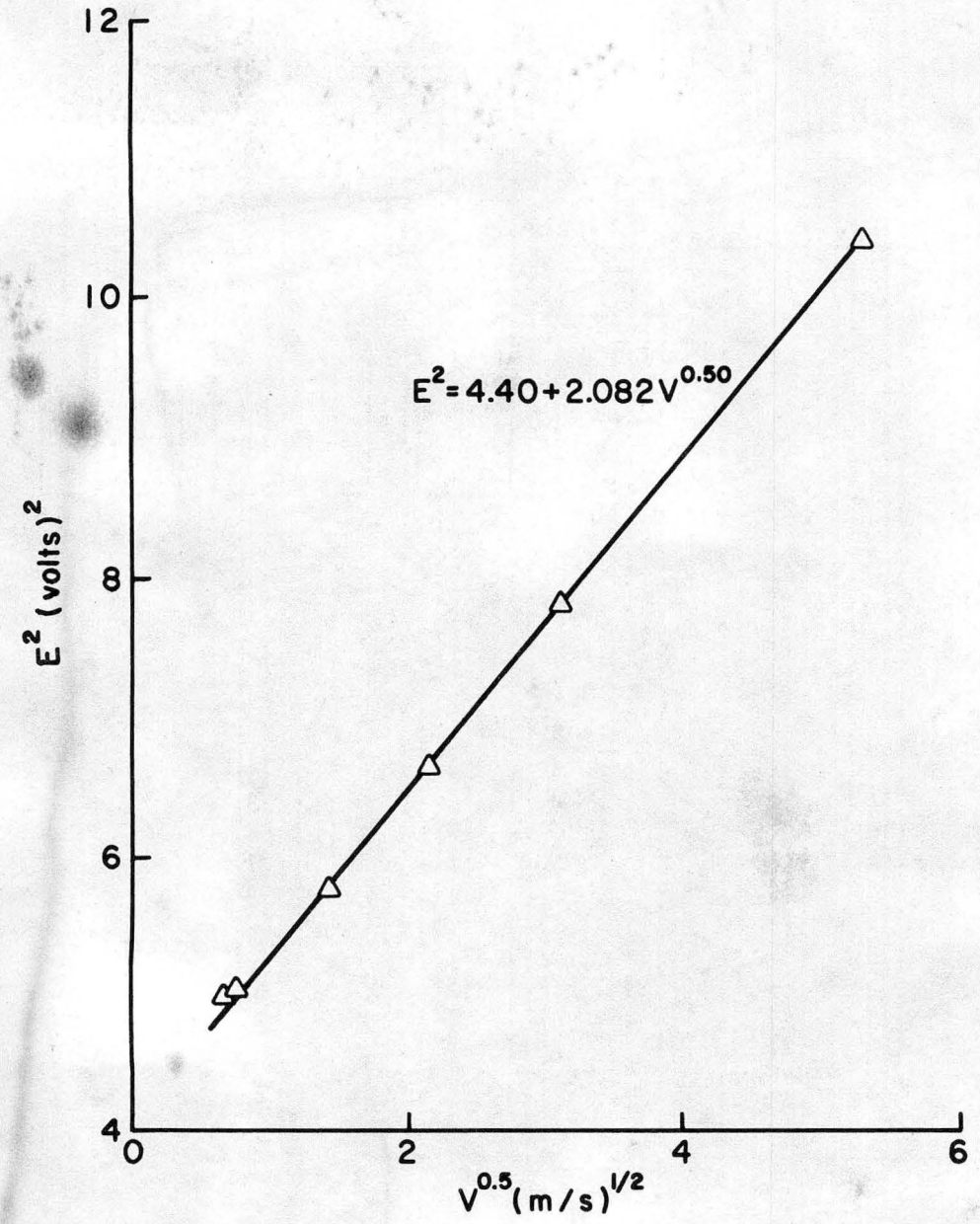

Figure 3.5-1. Calibration curve for the TSI hot-wire anemometer.

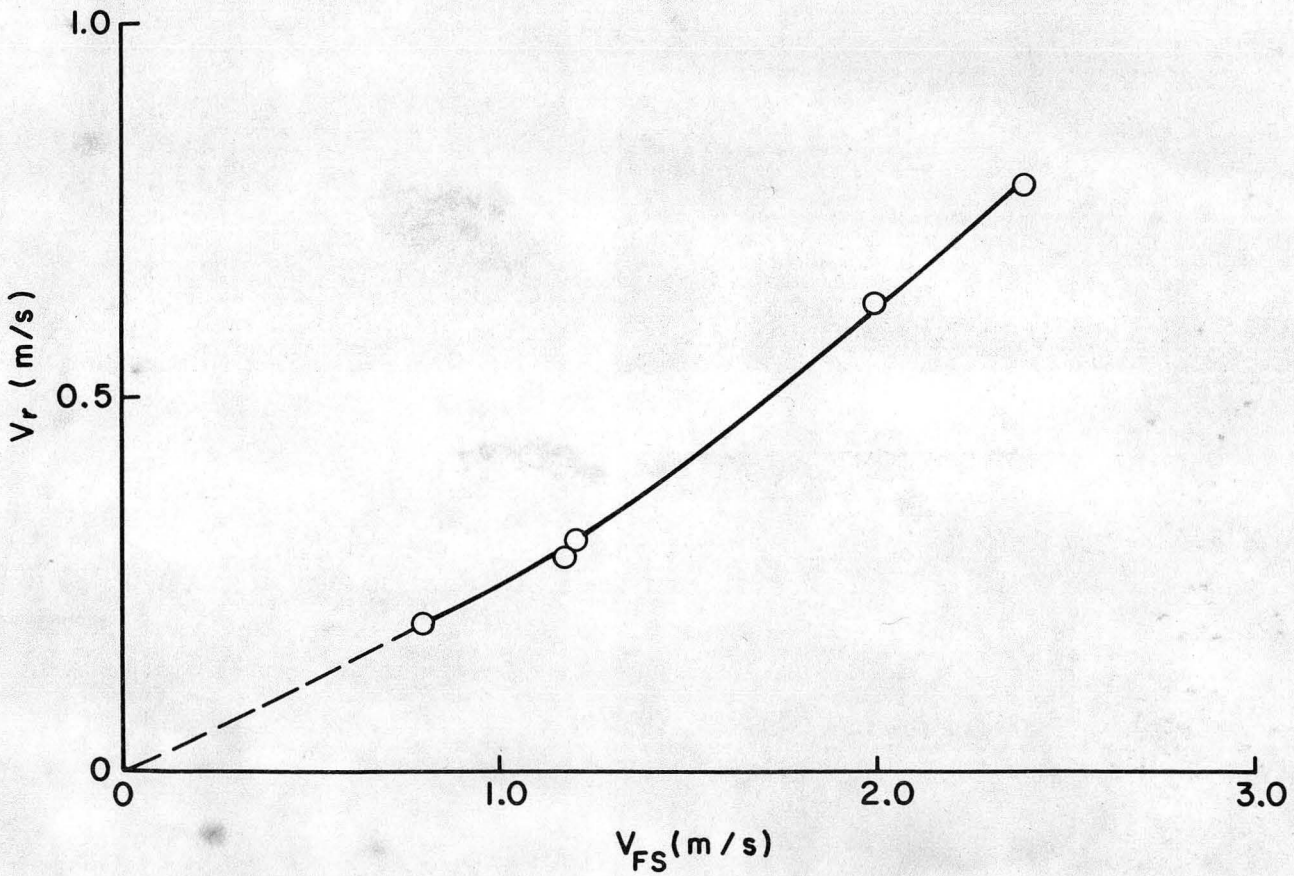

Figure 3.5-2. Freestream velocity versus velocity at the top of the meteorological tower in the Environmental Wind Tunnel for the 270° wind direction.

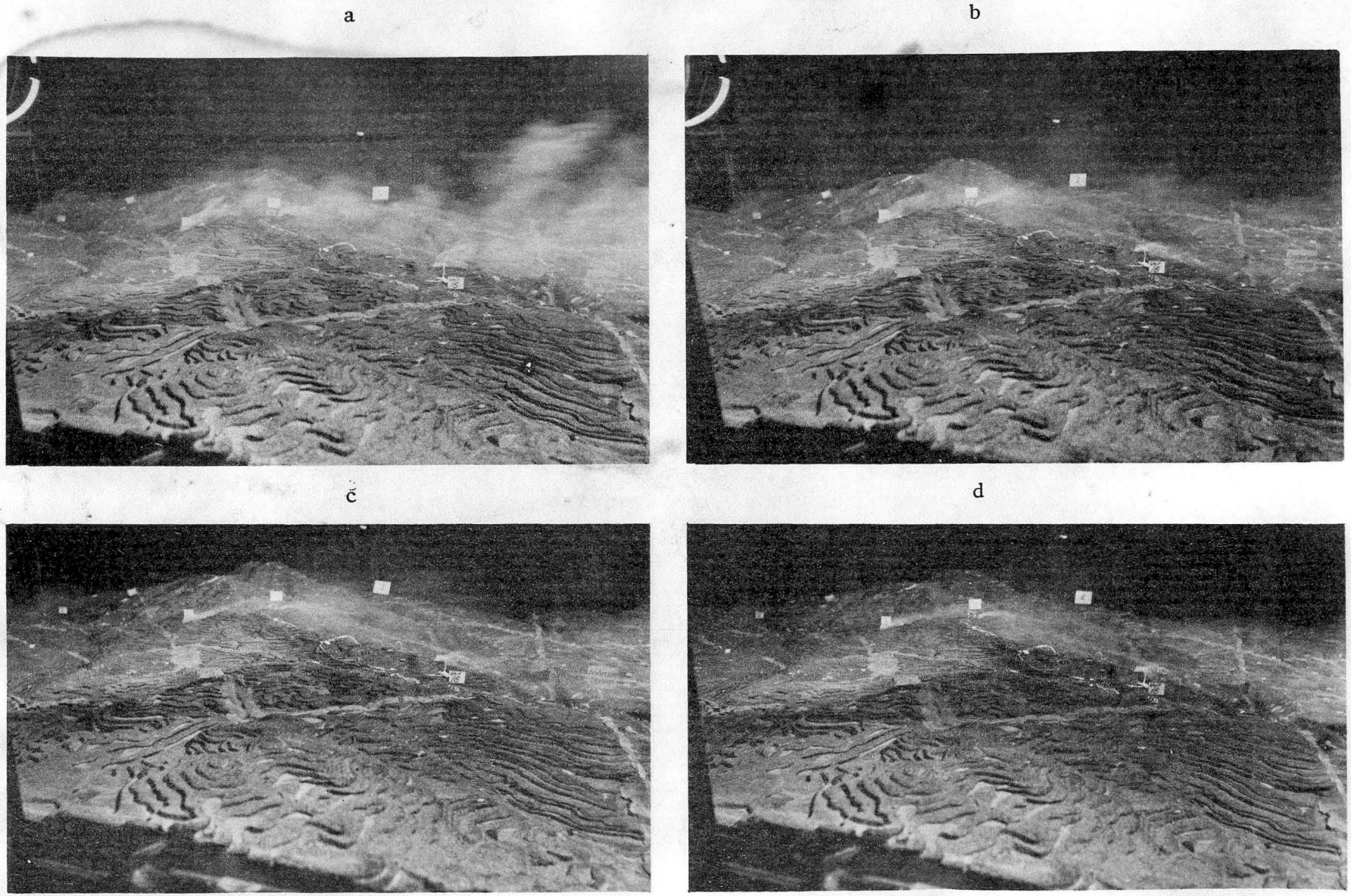

Figure 4.1. Plume visualization for units 13, 14, 16 and 18 for wind speeds of a) 2.5, b) 4.1, c) 7.8 and d) 10.9 m/s.

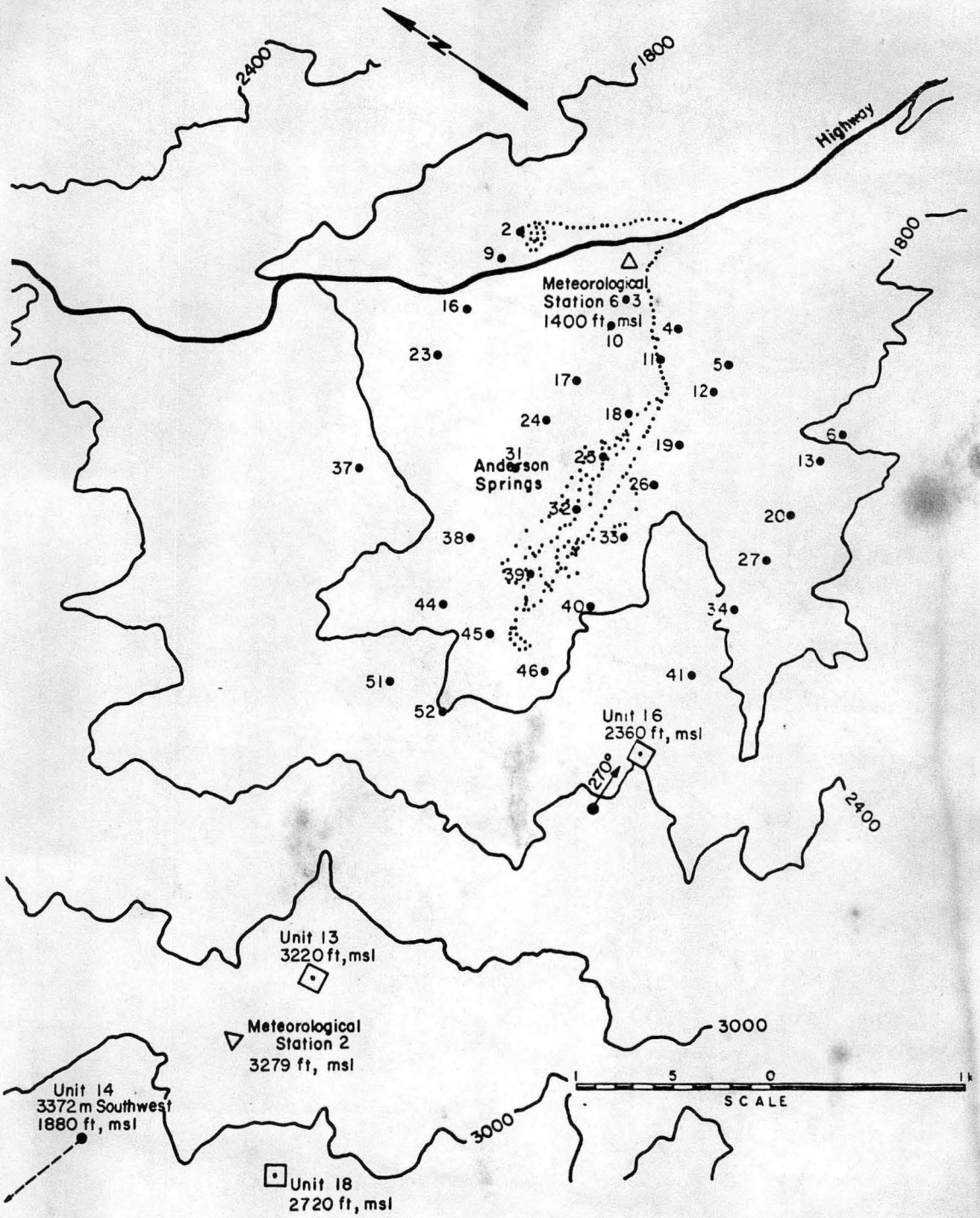

Figure 5.1. Sampling location key.

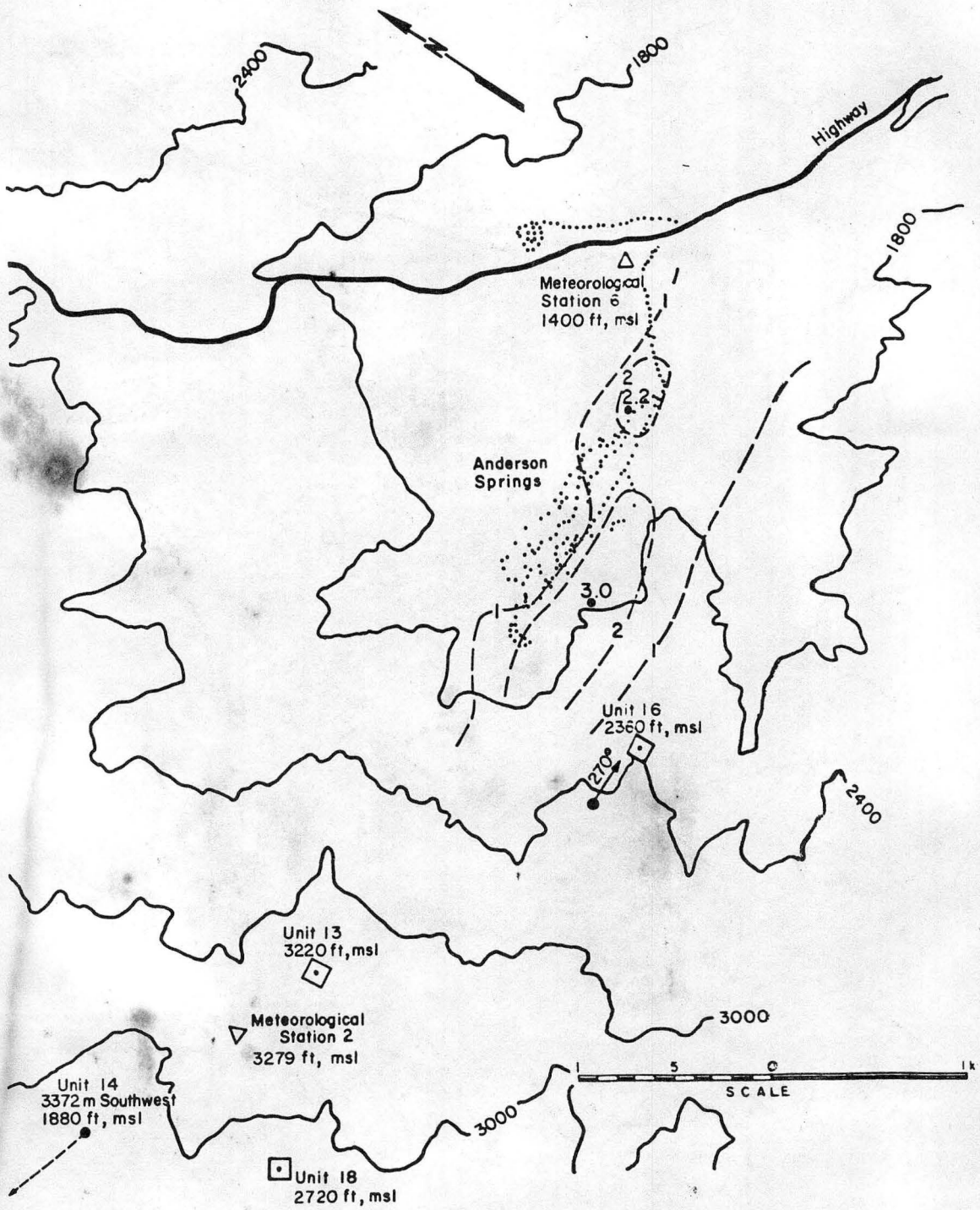

Figure 5.2a. Isopleths (x 10^5) of nondimensional concentration coefficient K for unit 13 and a wind speed of 2.5 m/s.

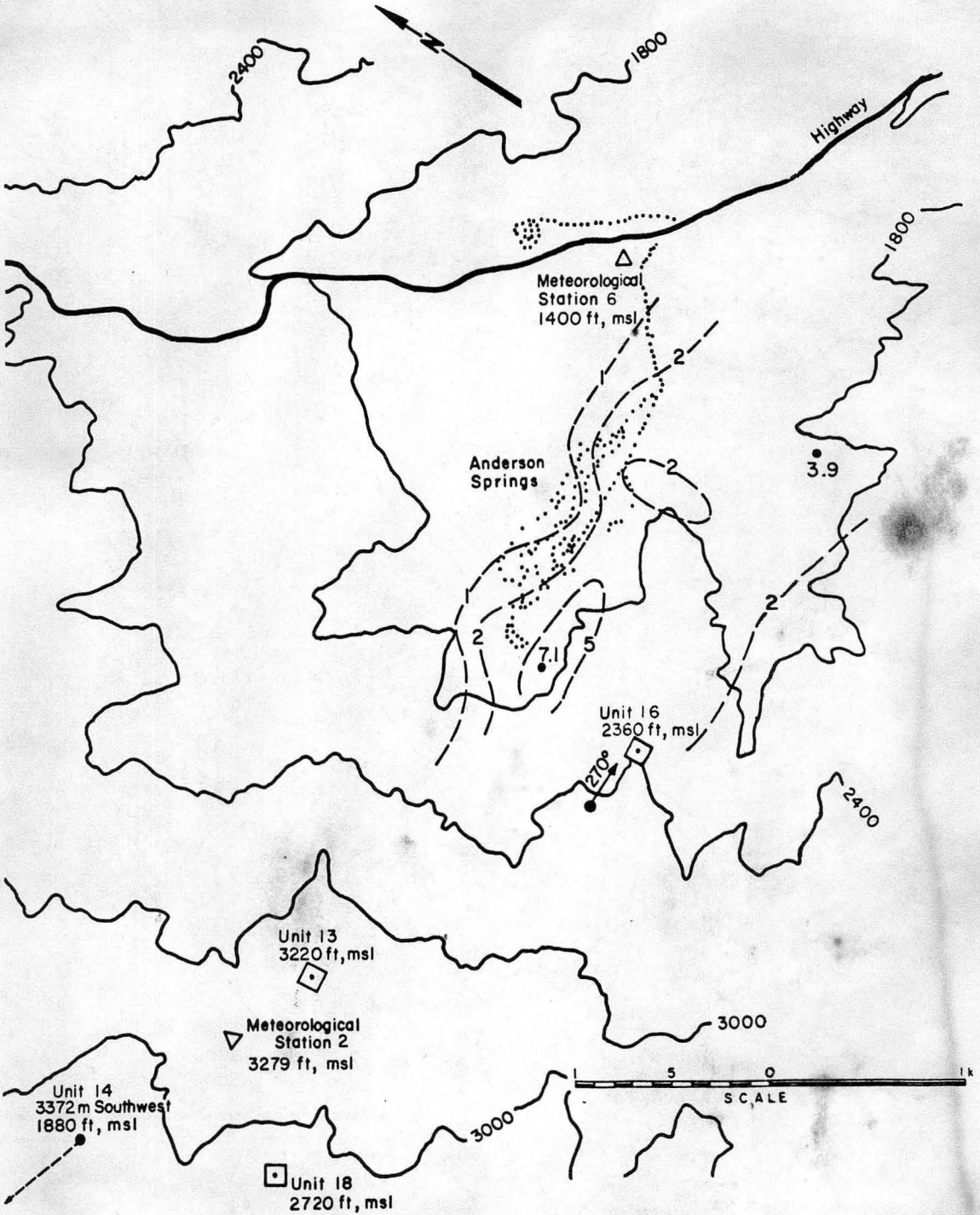

Figure 5.2b. Isopleths (x 10^5) of nondimensional concentration coefficient K for unit 13 and a wind speed of 4.1 m/s.

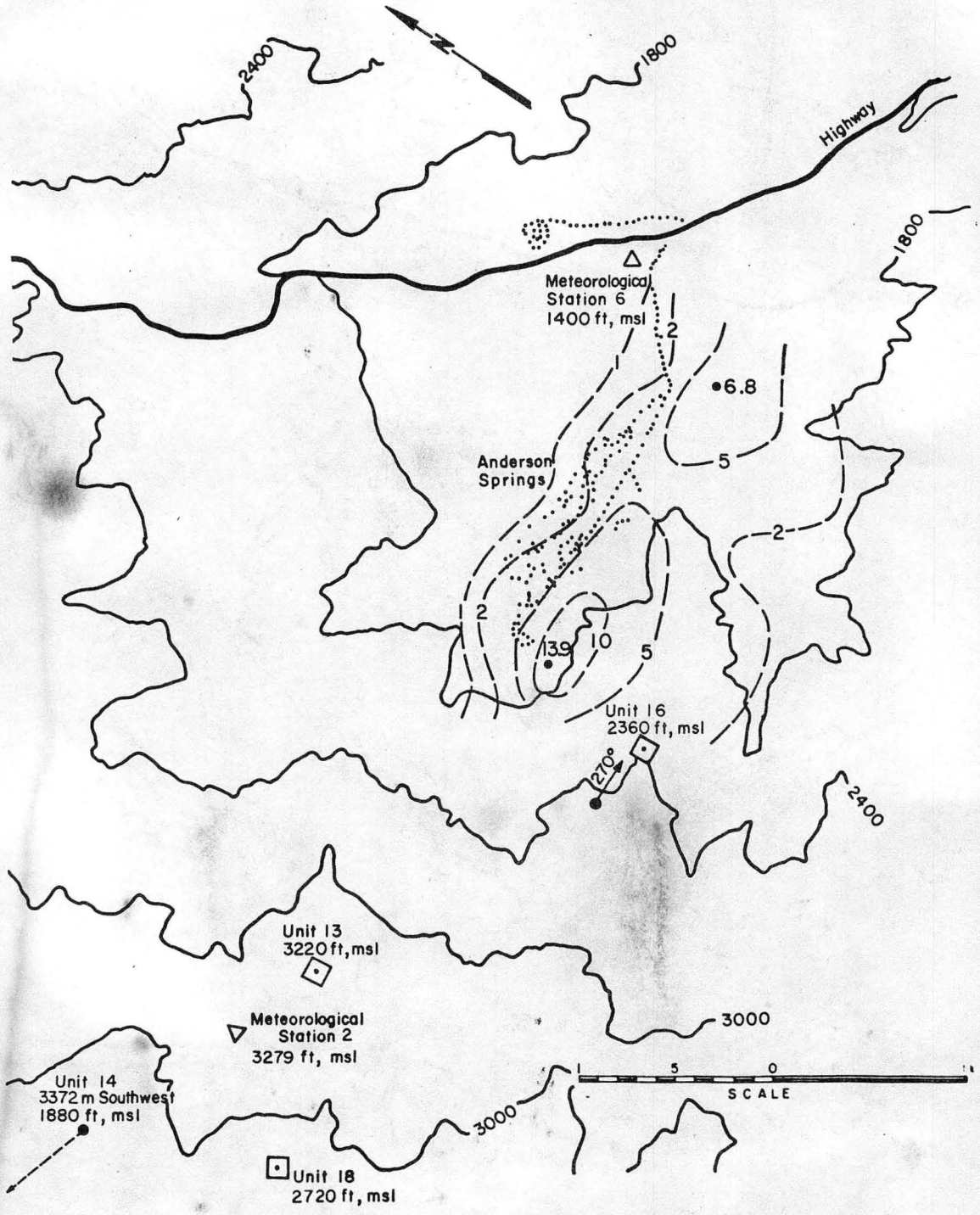

Figure 5.2c. Isopleths (x 10^5) of nondimensional concentration coefficient K for unit 13 and a wind speed of 7.8 m/s.

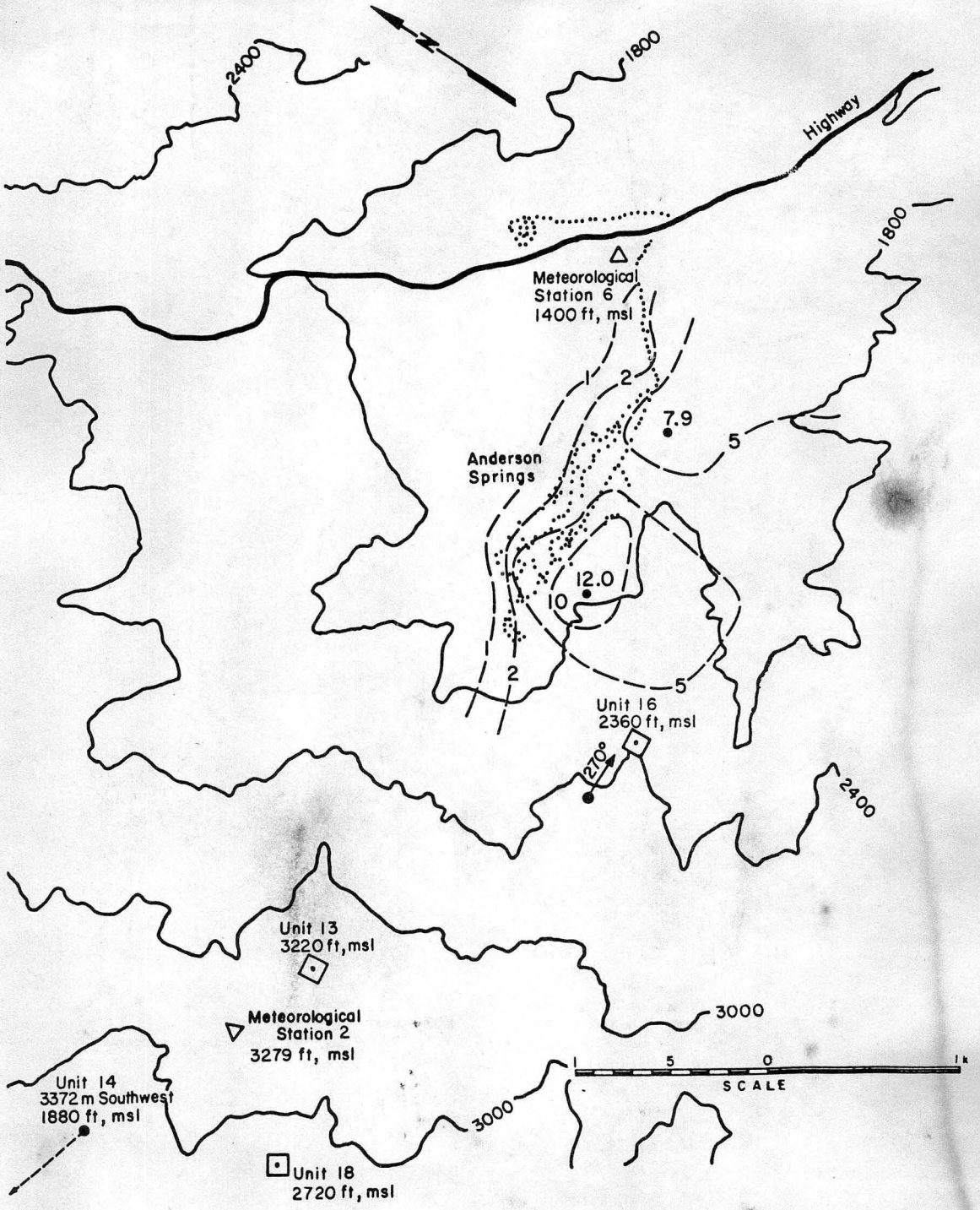

Figure 5.2d. Isopleths (x 10^5) of nondimensional concentration coefficient K for unit 13 and a wind speed of 10.9 m/s.

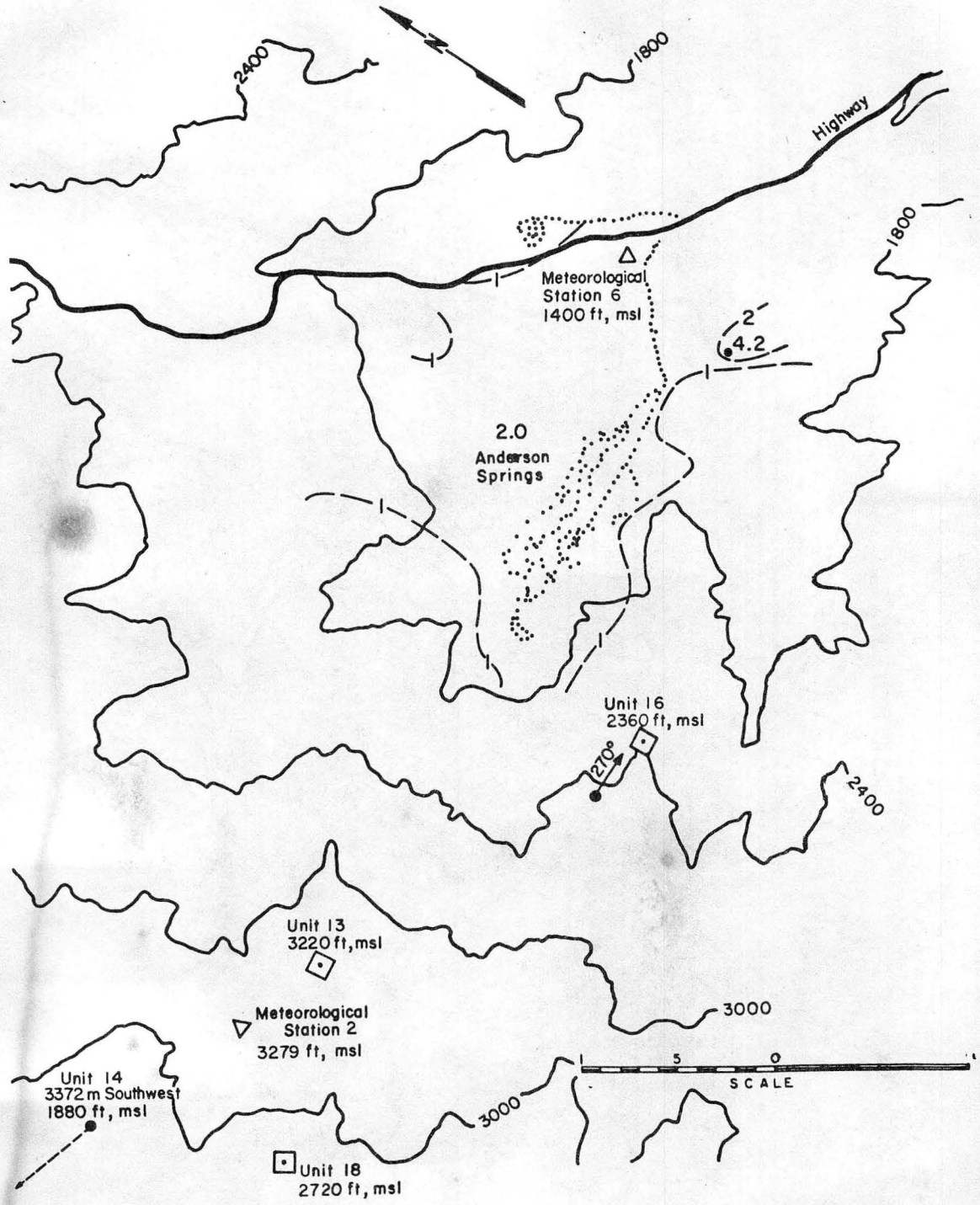

Figure 5.3a. Isopleths ($\times 10^{5}$) of nondimensional concentration coefficient K for unit 14 and a wind speed of 2.5 m/s.

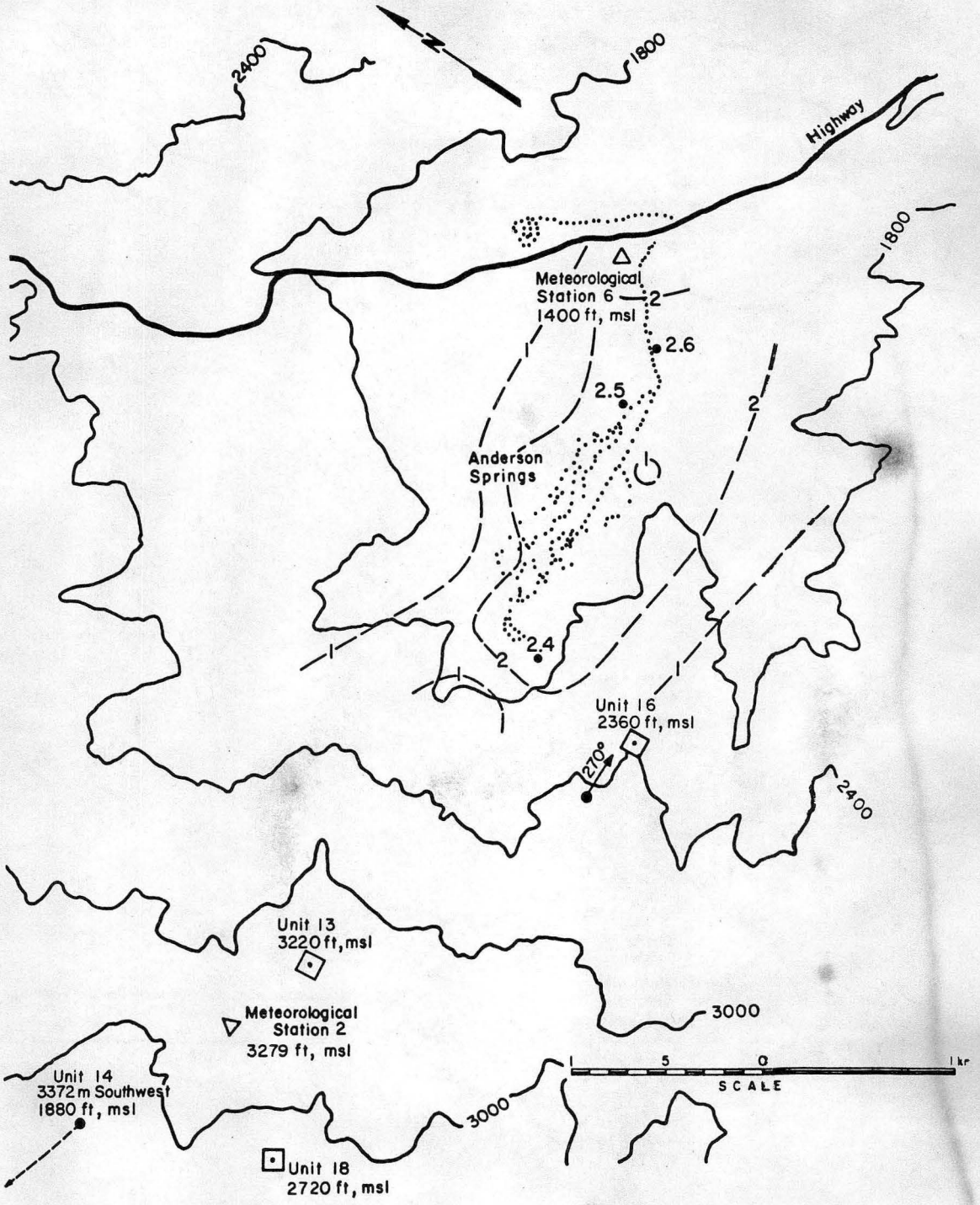

Figure 5.3b. Isopleths (x 10^5) of nondimensional concentration coefficient K for unit 14 and a wind speed of 4.1 m/s.

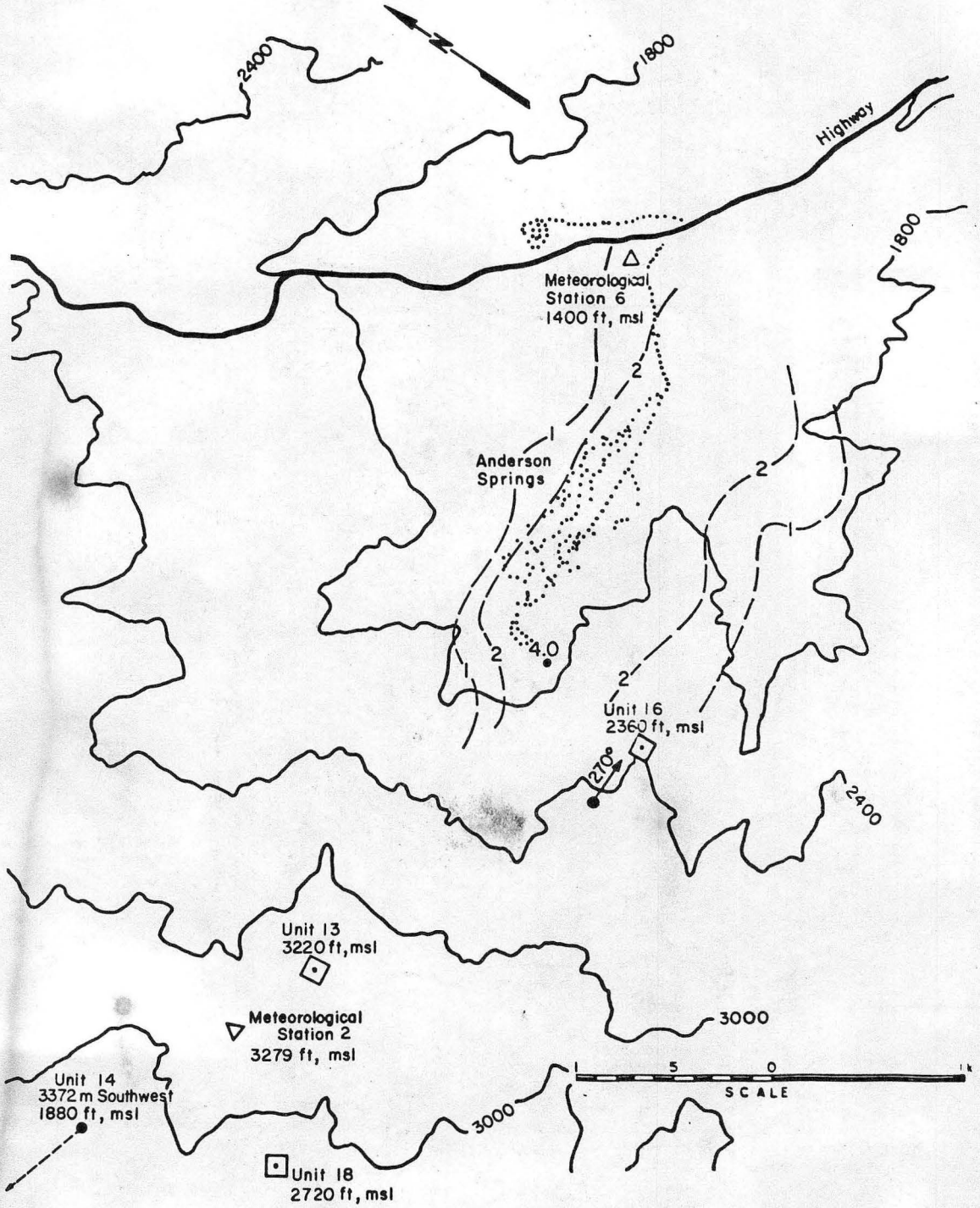

Figure 5.3c. Isopleths (x 10^5) of nondimensional concentration coefficient K for unit 14 and a wind speed of 7.8 m/s.

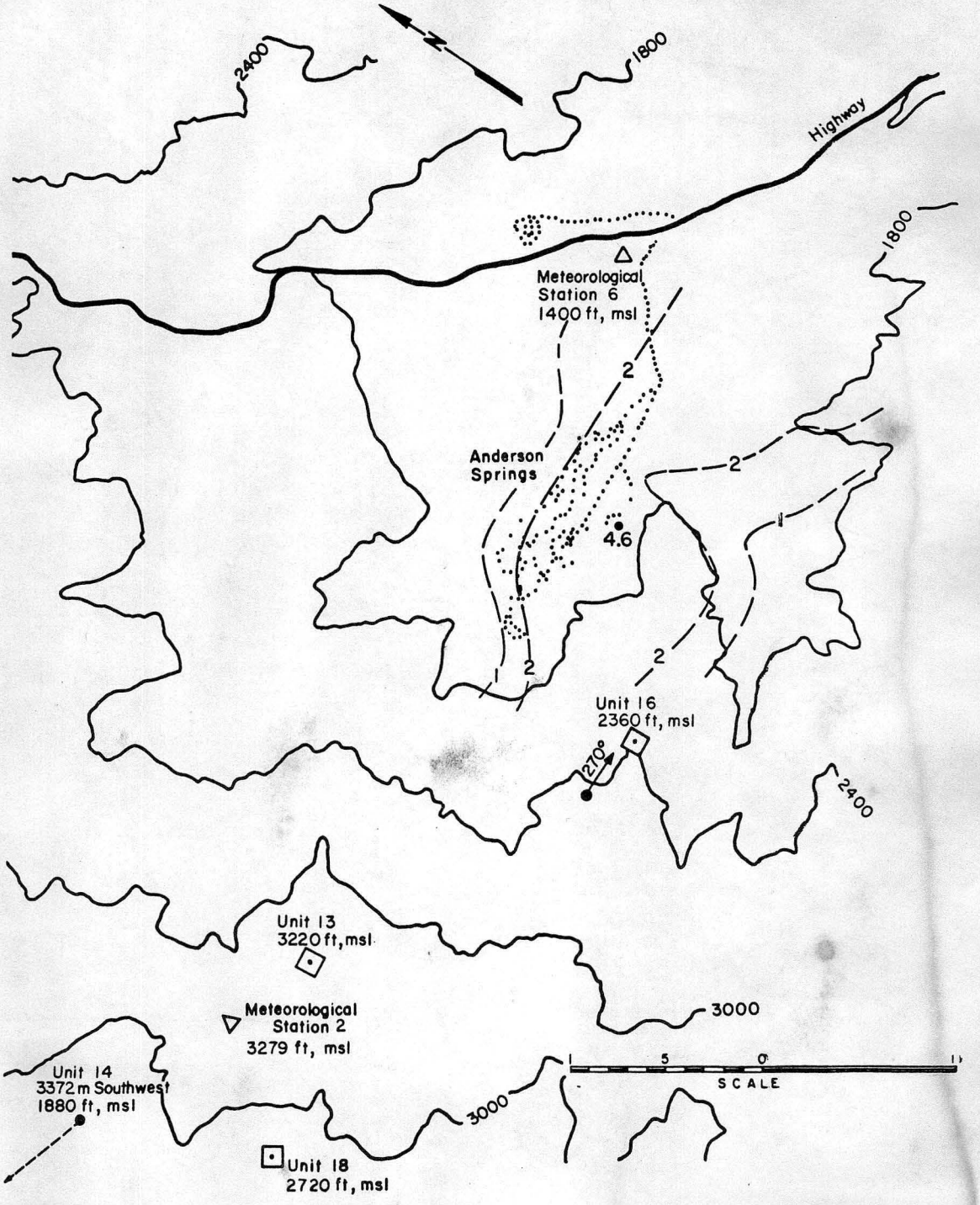

Figure 5.3d. Isopleths (x 10^5) of nondimensional concentration coefficient K for unit 14 and a wind speed of 10.9 m/s.

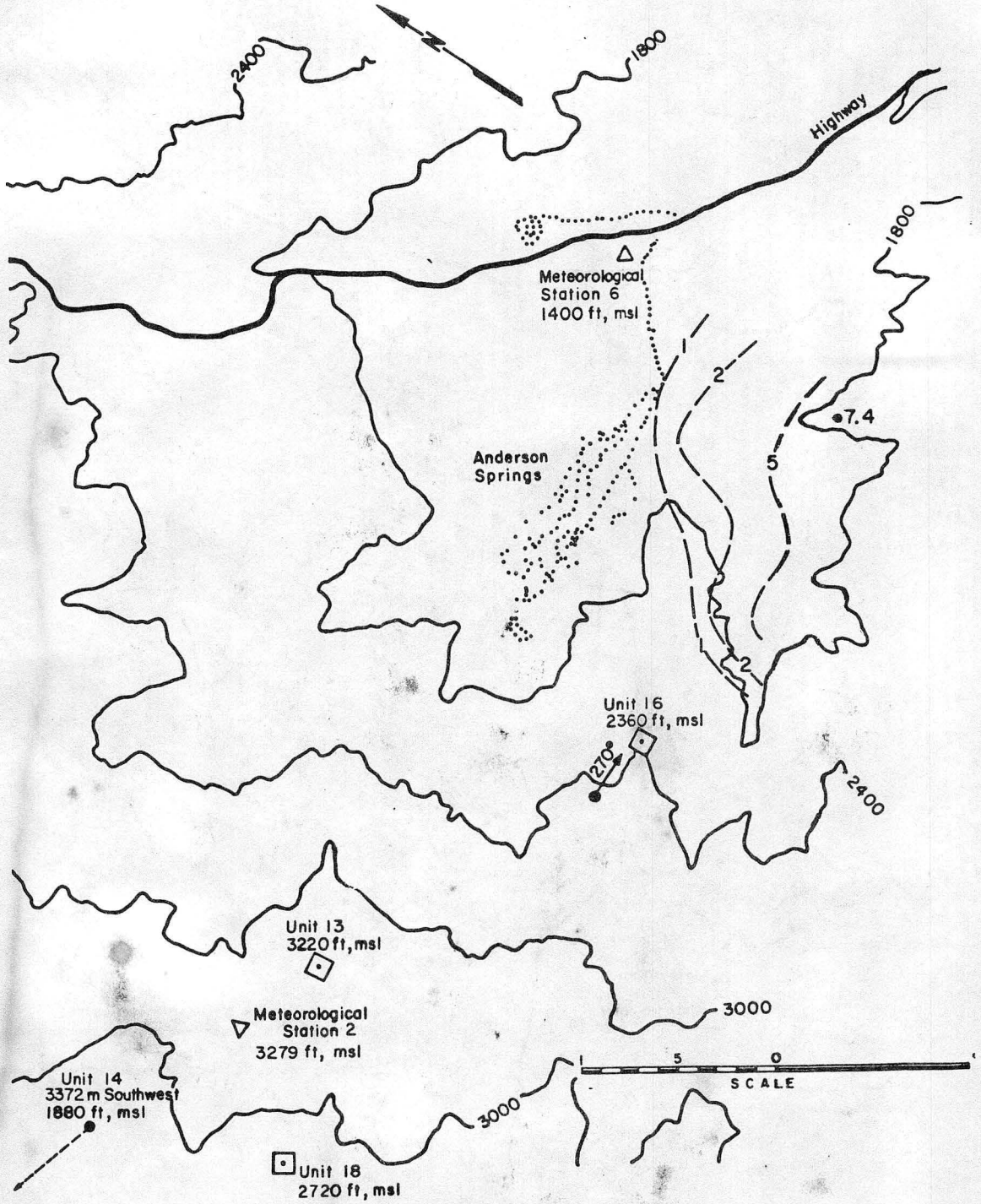

Figure 5-4a. Isopleths (x 10^5) of nondimensional concentration coefficient K for unit 16 and a wind speed of 2.5 m/s.

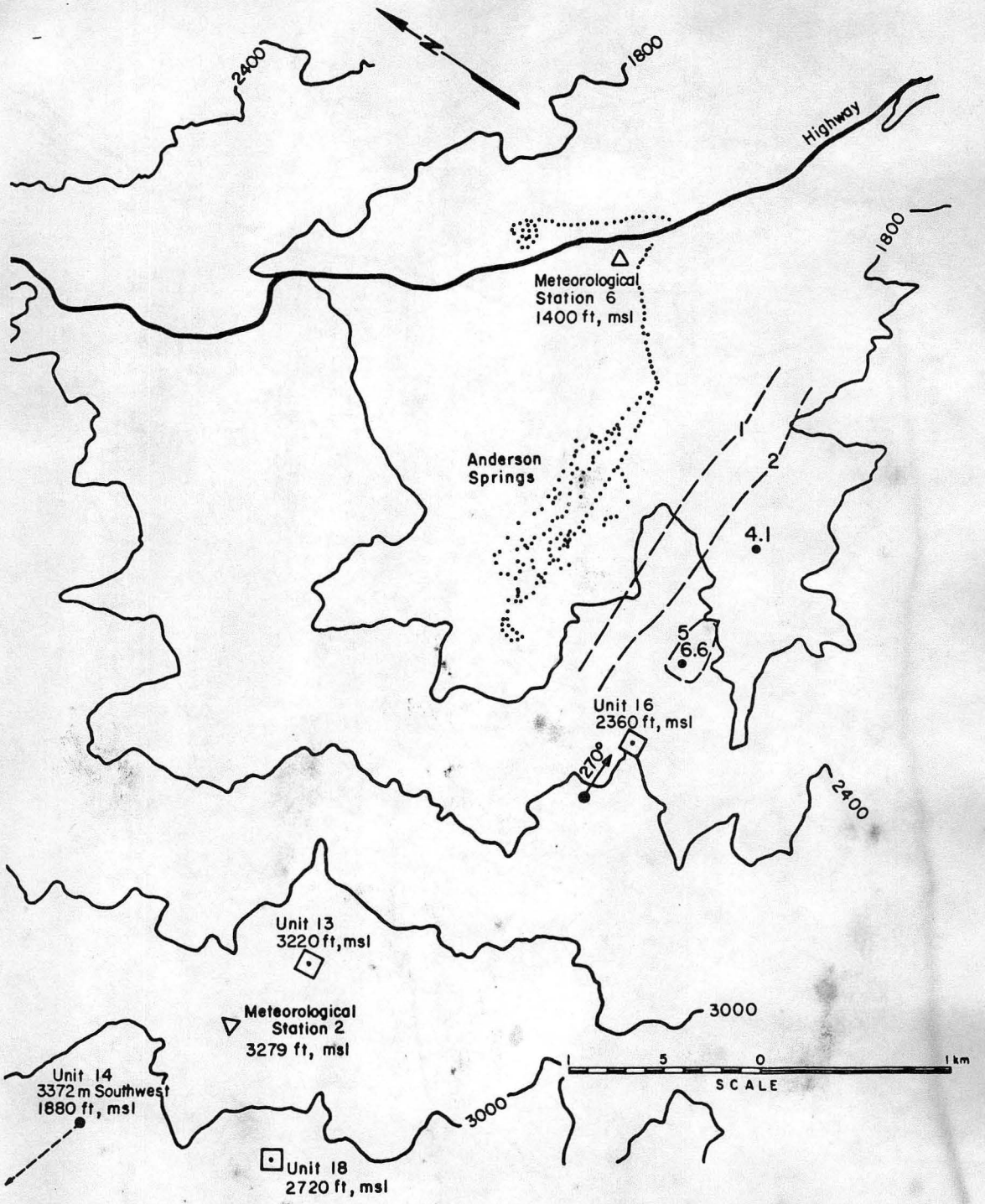

Figure 5.4b. Isopleths (x 10^5) of nondimensional concentration coefficient K for unit 16 and a wind speed of 4.1 m/s.

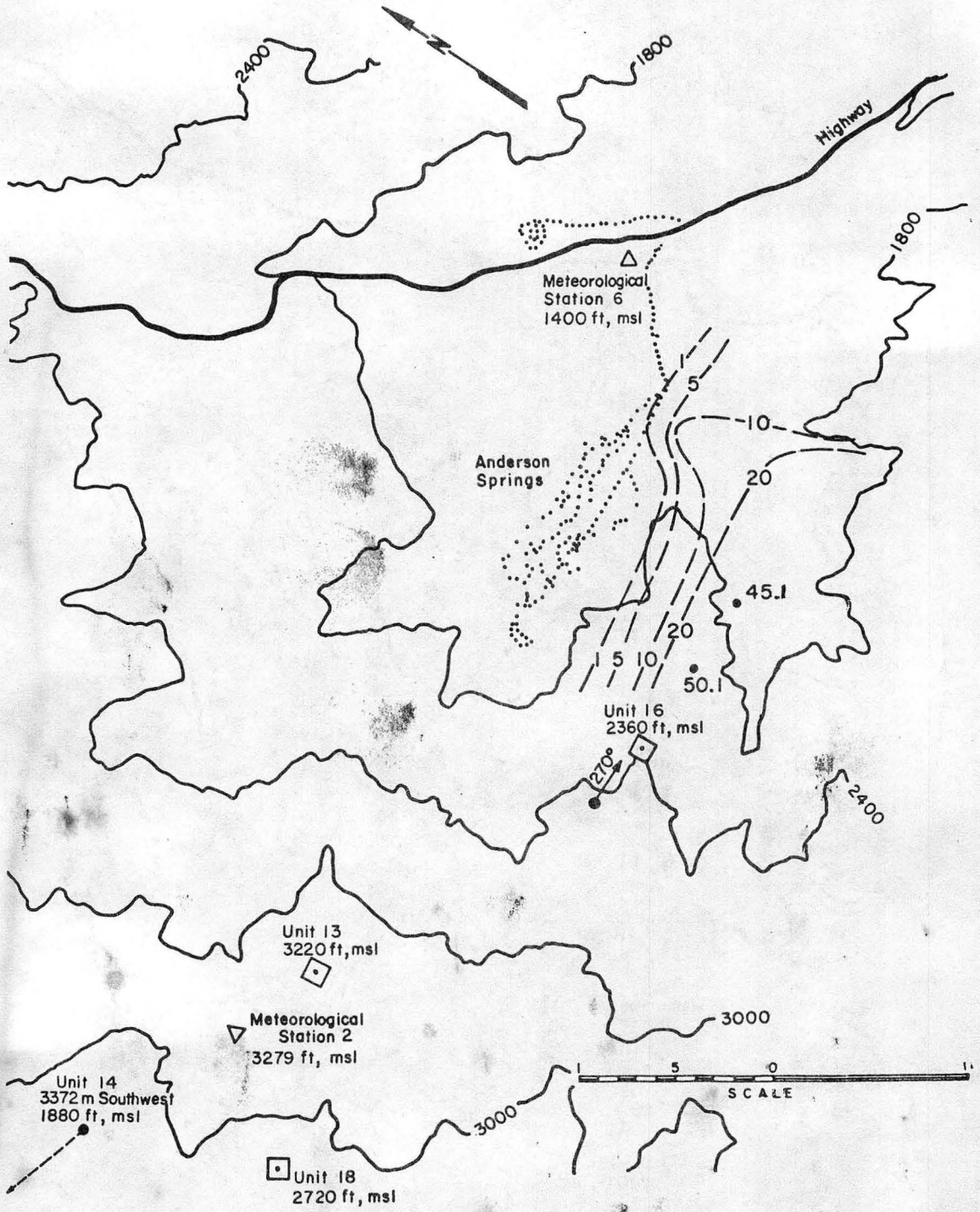

Figure 5.4c. Isopleths (x 10^5) of nondimensional concentration coefficient K for unit 16 and a wind speed of 7.8 m/s.

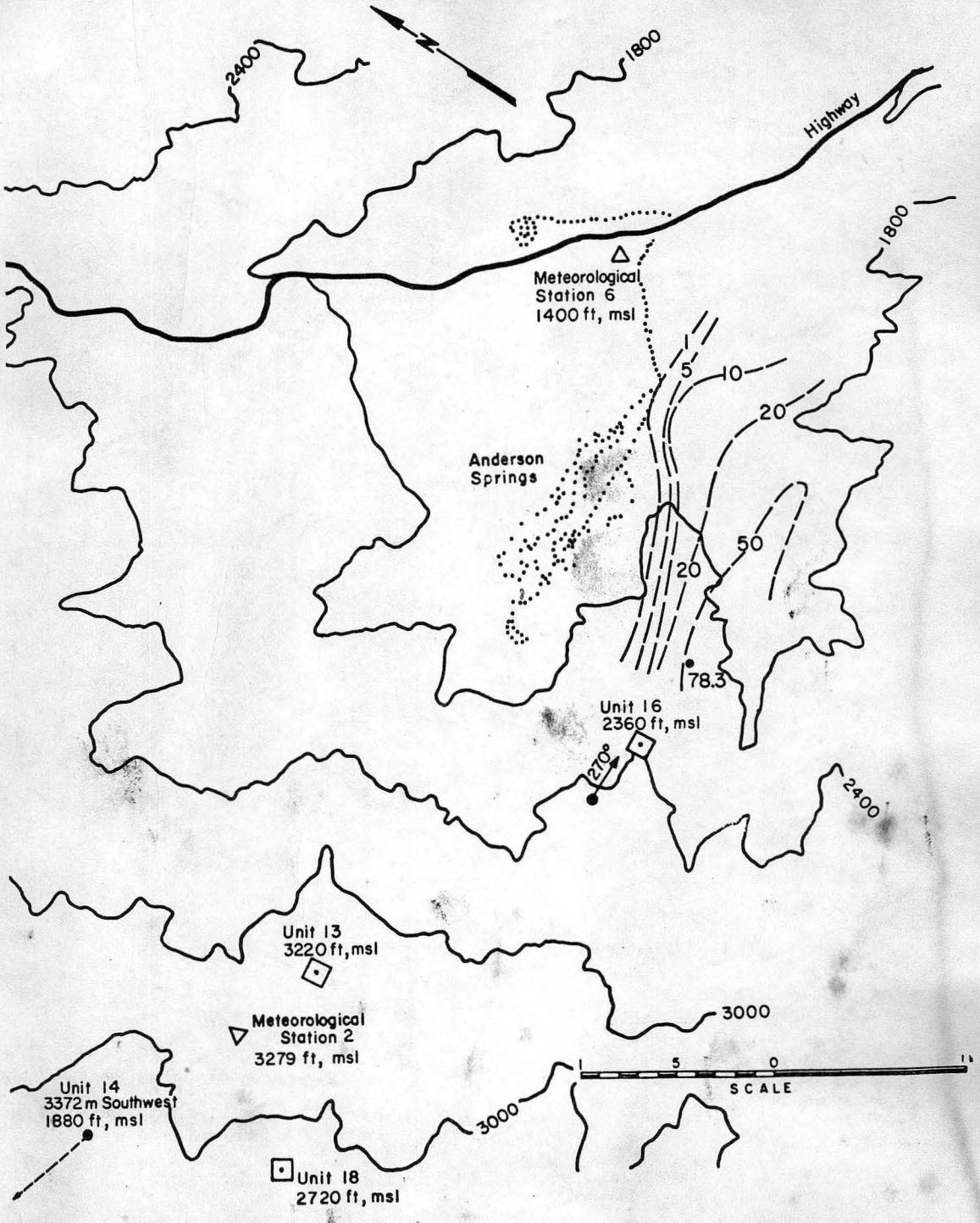

Figure 54.d. Isopleths (x 10^5) of nondimensional concentration coefficient K for unit 16 and a wind speed of 10.9 m/s.

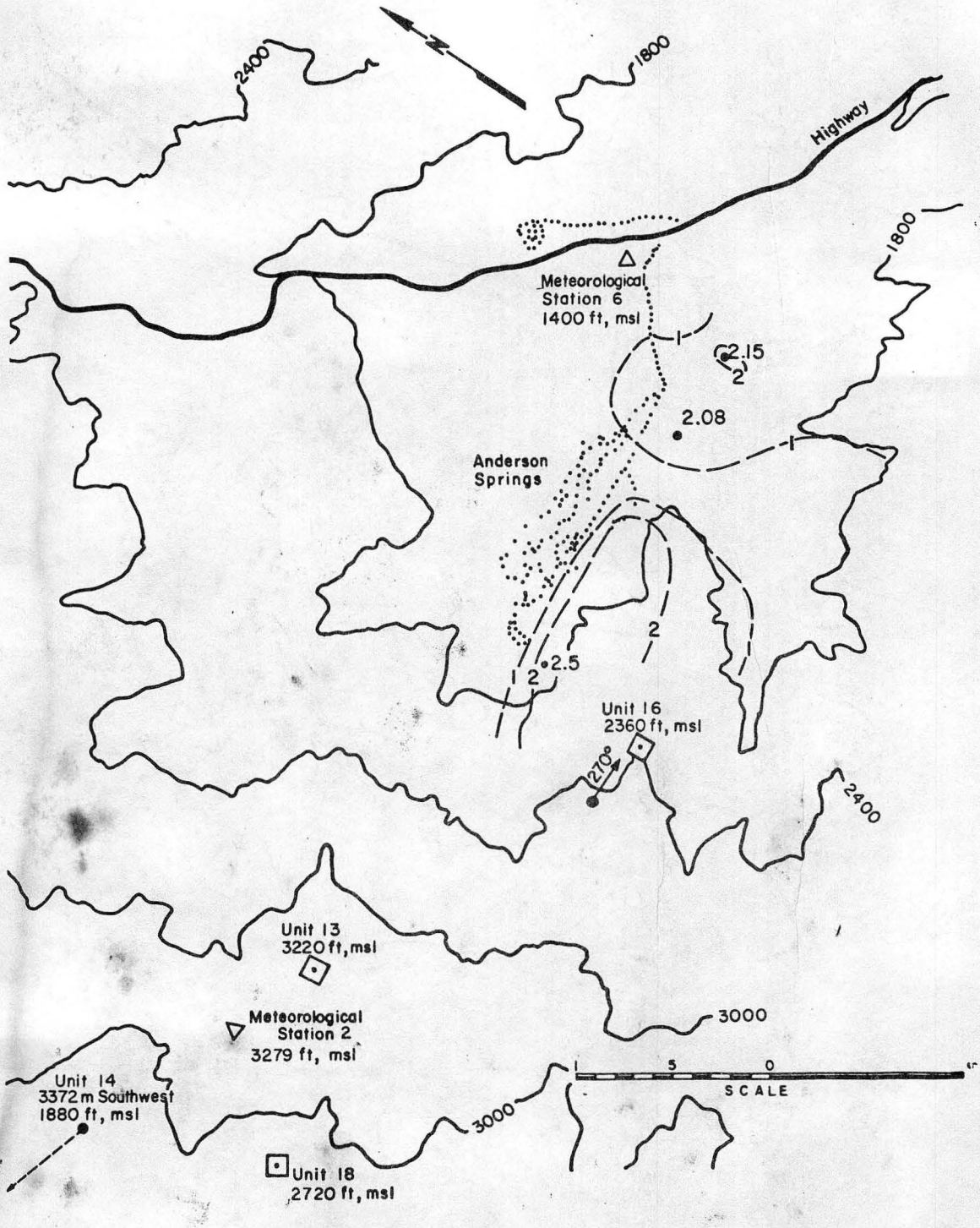

Figure 5.5a. Isopleths (x 10^5) of nondimensional concentration coefficient K for unit 18 and a wind speed of 2.5 m/s.

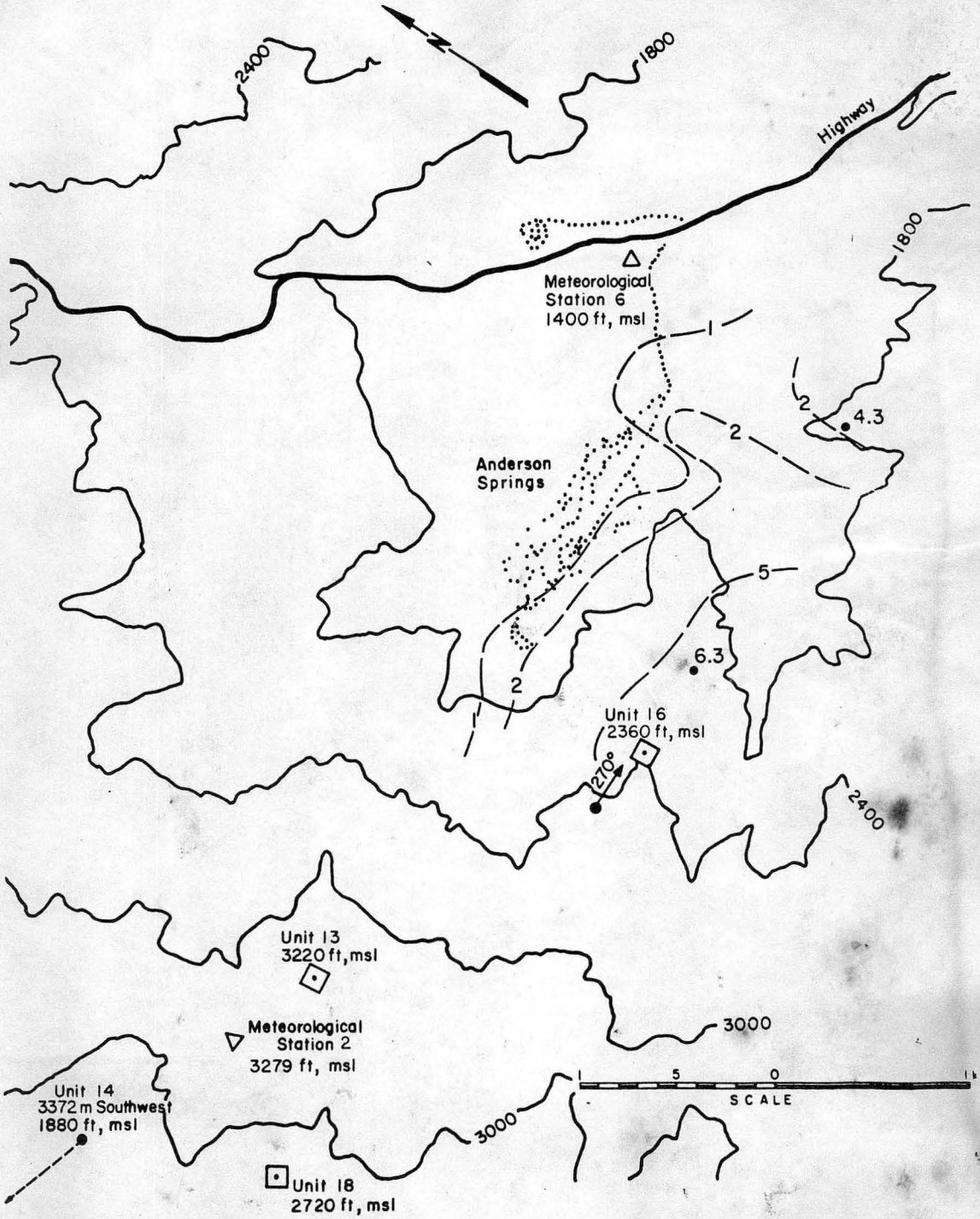

Figure 5.5b. Isopleths (x 10^5) of nondimensional concentration coefficient K for unit 18 and a wind speed of 4.1 m/s.

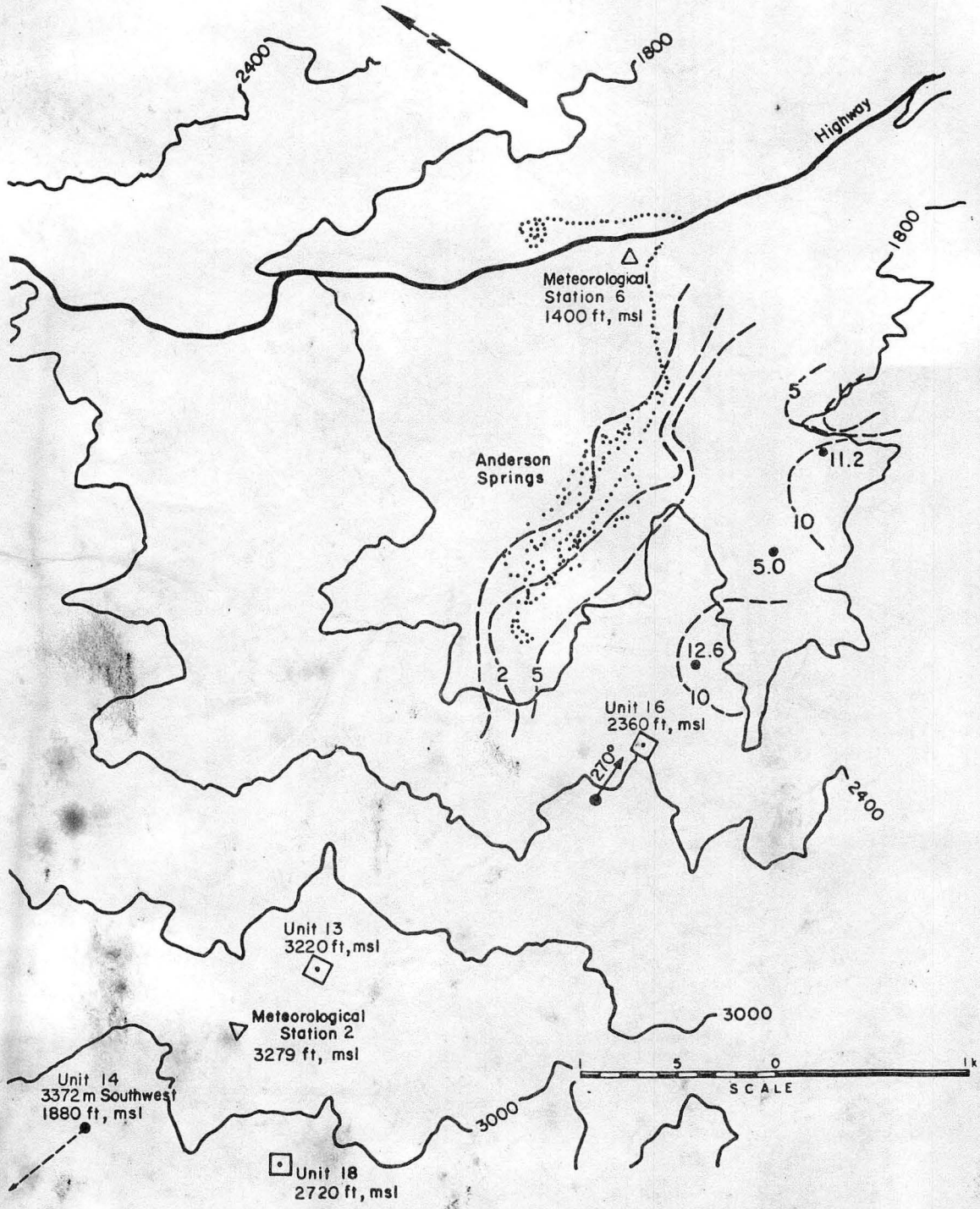

Figure 5.5c. Isopleths (x 10^5) of nondimensional concentration coefficient K for unit 18 and a wind speed of 7.8 m/s.

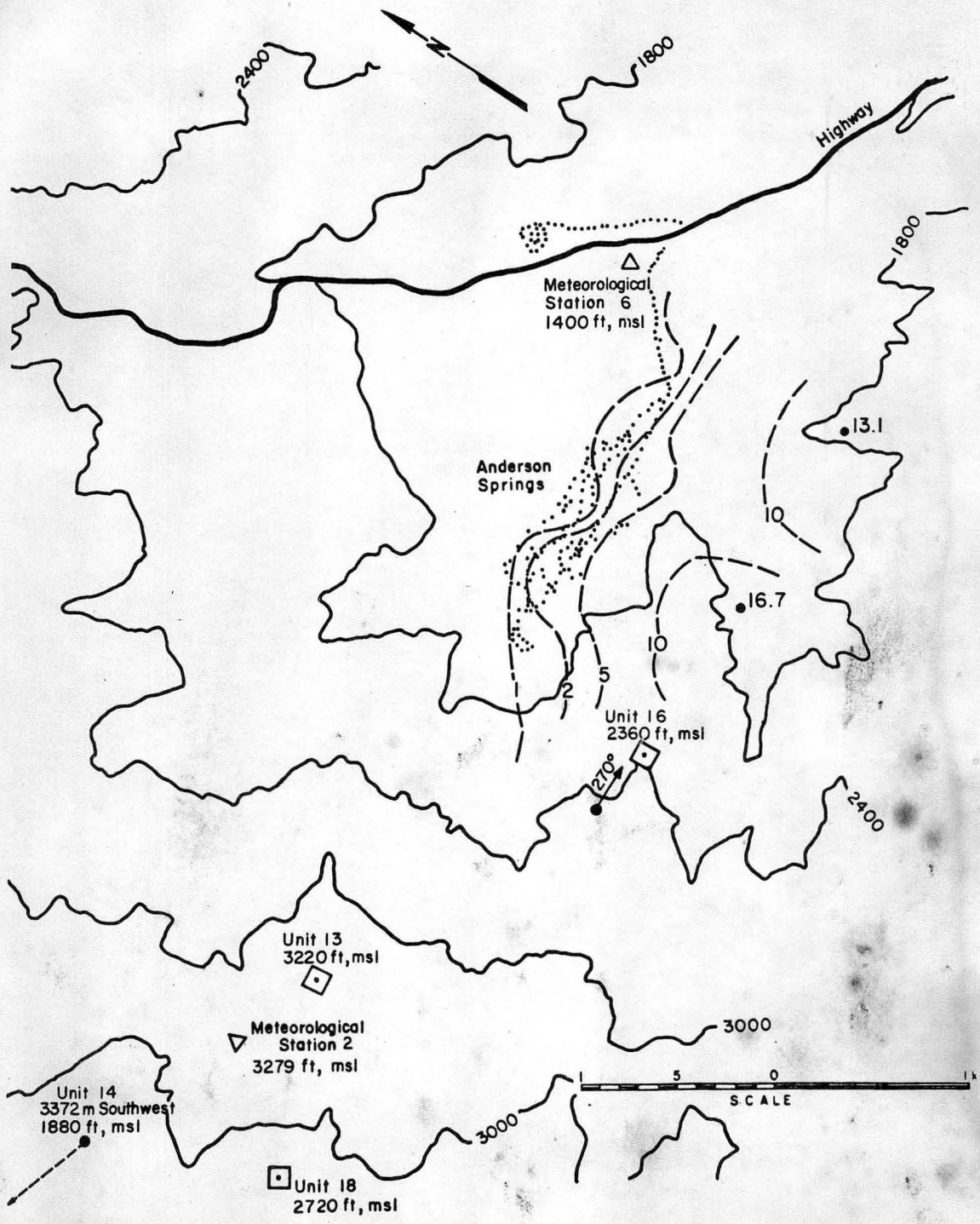

Figure 5.5d. Isopleths (x 10^5) of nondimensional concentration coefficient K for unit 18 and a wind speed of 10.9 m/s.

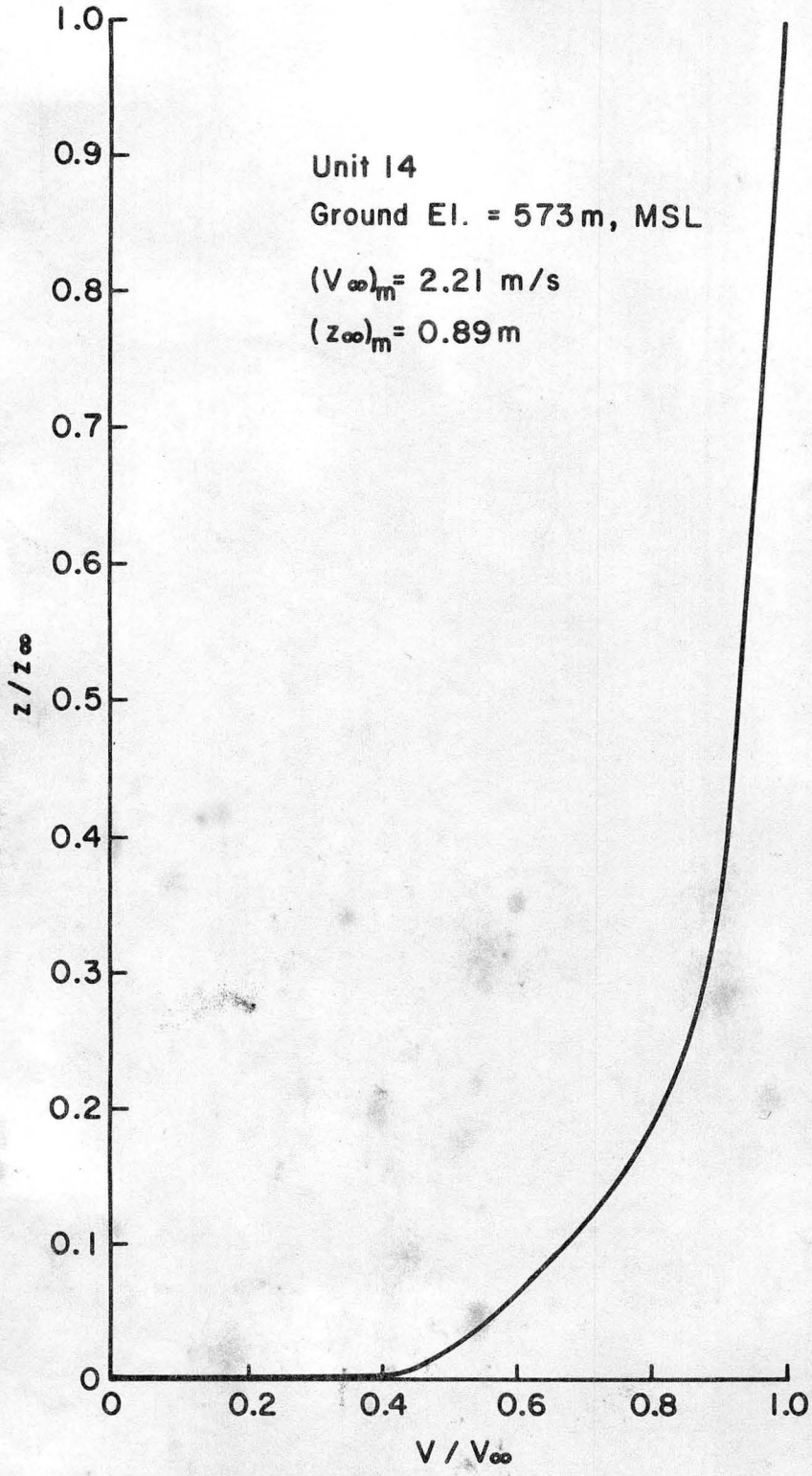

Figure 6.1b. Velocity profile above unit 14.

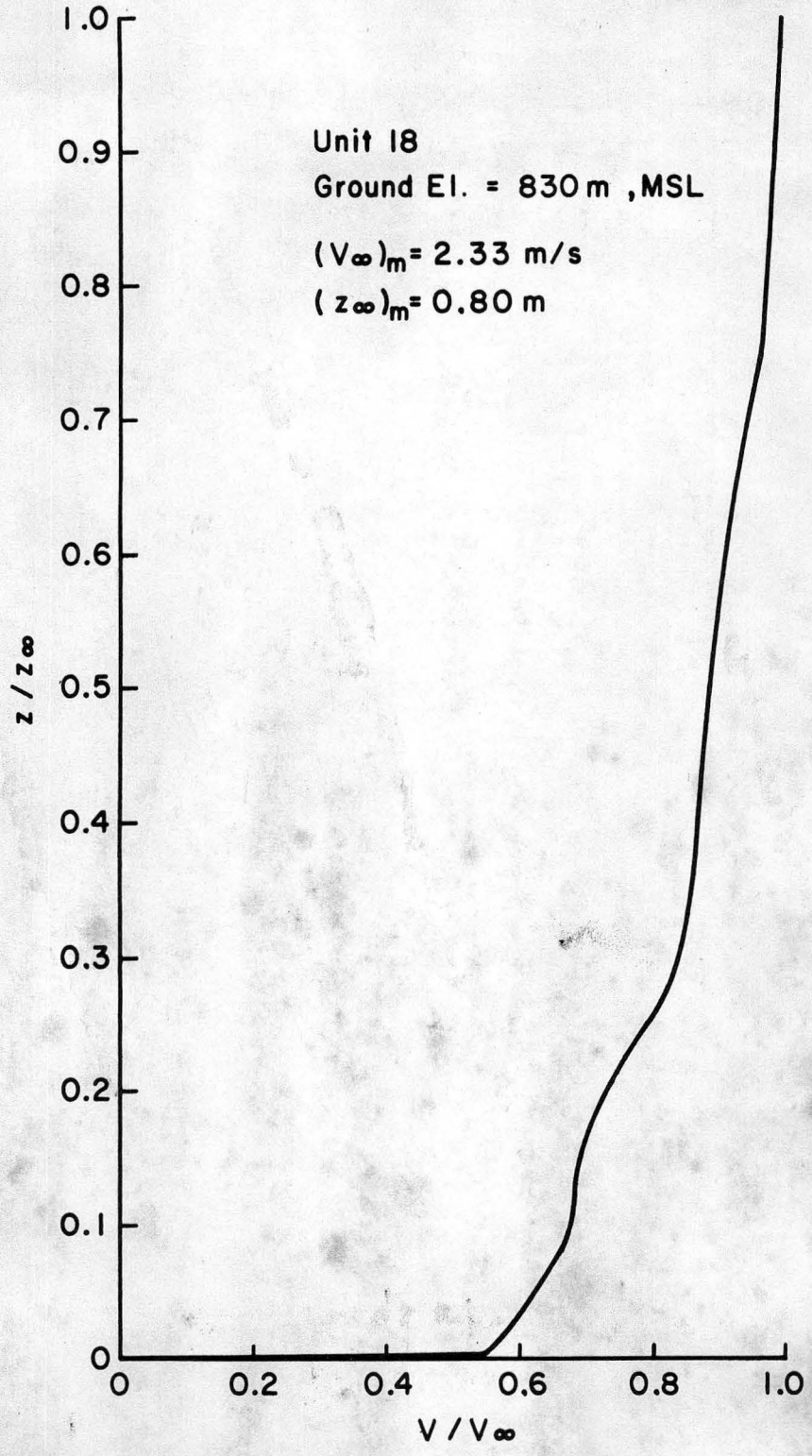

Figure 6.1c. Velocity profile above unit 18.

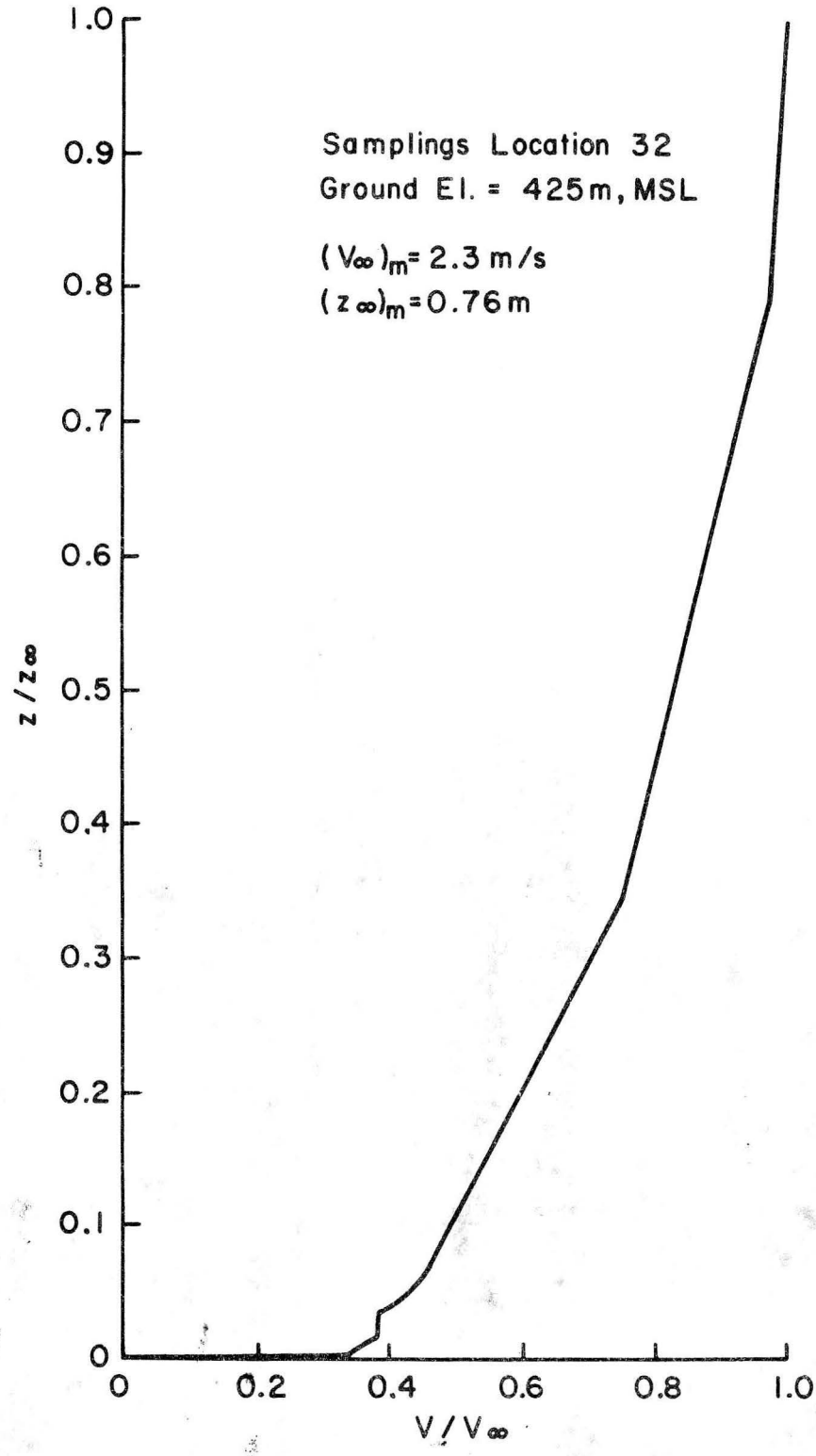

Figure 6.1d. Velocity profile above Anderson Springs (sampling grid location 32).

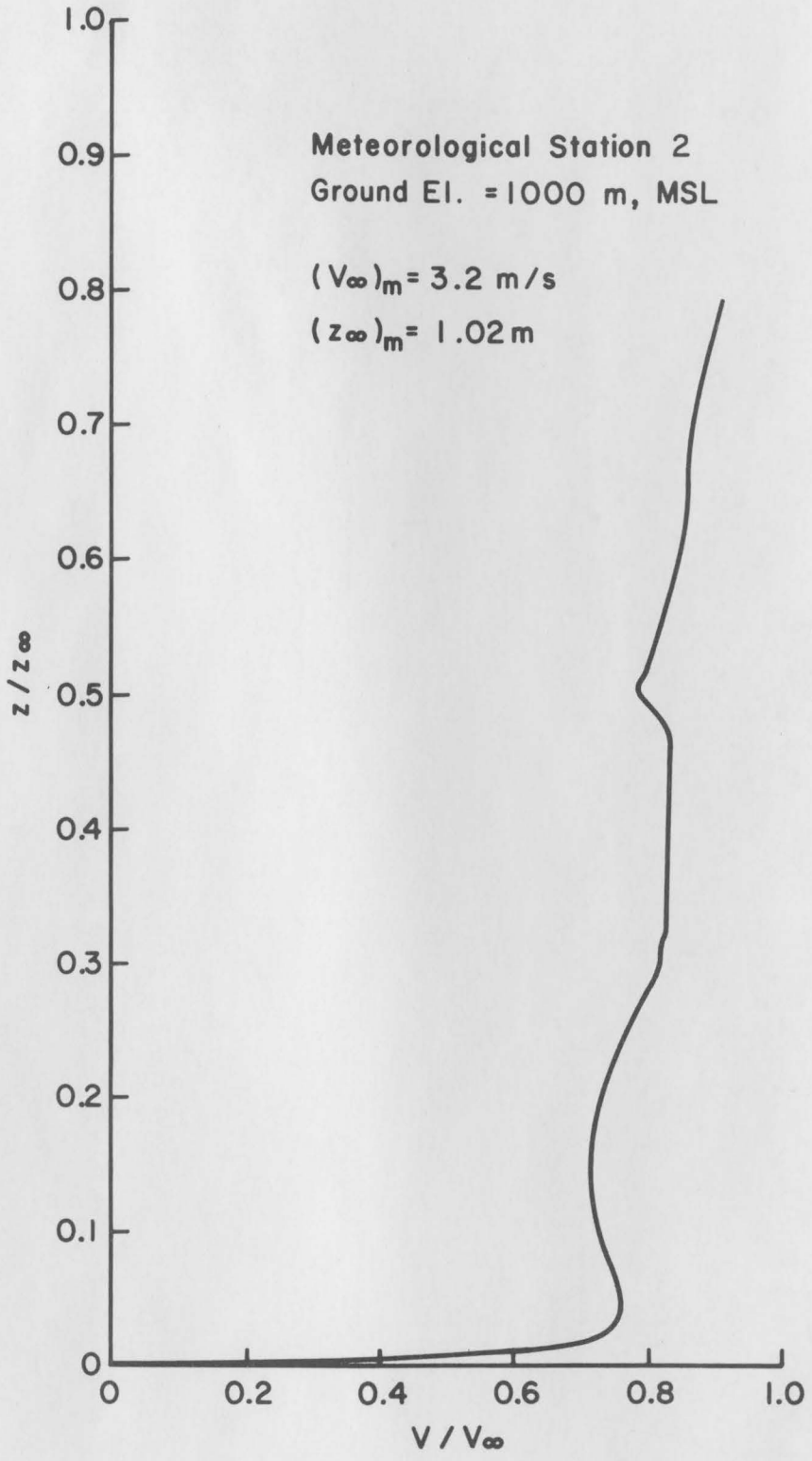

Figure 6.1a. Velocity profile above the meteorological tower, Station 2 (Anderson Ridge).